2

# PIONEER PLASMA PROBE INSTRUMENT SIMULATION STUDY

By Grace Wahba

November, 1970



Prepared under Contract No. NAS2-5233 by

Grace Wahba, Ph.D.
3300 Tally Ho Lane
Madison, Wisconsin, 53705

Wisconsin Univ, Madison

for

AMES RESEARCH CENTER

NATIONAL AERONAUTICS AND SPACE ADMINISTRATION

TABLE OF CONTENTS



Figures for each Section follow the Section

## SECTION 0.

## SUMMARY

This is the written portion of work performed uncer NASA Contract NAS2-5233 - "Report on Pioneer's 6/7 Plasma Probe Instrument Simulation Study." In response to the direction of the Technical Monitor, this report concentrates on part A.1.(2) of the work statement "recommendations concerning the design and construction of a second generation version of this algorithm ..." The recommendations contained herein are designed to be applicable to the analysis of data from the later 3 Collector Electrostatic Analyzer System. As per the contract, a minimum of six days were spent in consultation with Ames Scientists during the summer of 1970.

The results of three independent studies are reported here. They are 1.) Optimization of Numerical Quadratures in the Plasma Probe Non-Linear Least Squares Parameter Estimation Program, 2.) An Alternative Technique for Estimating the Helium Fraction and 3.) Linear Estimates of the Plasma Parameters.

# SECTION 1.

## INTRODUCTION

Effort on this contract has been concentrated on the development of techniques for estimating as many as possible of the (steady-state) plasma parameters, from data observed by Pioneer 9 type instruments. The basic technique for doing this for Pioneer 6 and 7 has involved a mathematical model of the instrument response, and a mathematical model of the solar wind particle velocity vector distribution, as a function of its parameters. A non-linear least squares algorithm in conjunction with these models, has been successfully used to estimate the parameters. Work under this contract has proceeded under the assumption that this basic technique is sound for 9 type instruments. The 9 instrument response functions are of somewhat different shape than those for Pioneer 6 and 7.

Loosely speaking, the $k^{th}$ data point $I_k$ is modeled as $I_k = I_k(\theta)$, where

$$I_k(\theta) = \iiint w_k(v) f(v;\theta) dv \ , \qquad (1.1)$$

$v$ is a velocity vector, $w_k(v)$ is the total instrument response to a unit number density cold beam with velocity vector $v$ at the $k^{th}$ choice of azimuth, collector, and energy step combination, and $f(v,\theta)$ is the particle velocity vector distribution, as a function of its $m$ parameters, $\theta = (\theta_1,\theta_2,\ldots,\theta_m)$. These parameters include the

components of the mean vector(s), and pressure tensor(s), number density, helium fraction, etc. $w_k(v)$ is obtained from the calibration data and the impulse response of the electronics.

The non-linear least squares program attempts to iteratively choose the parameter set $\theta = (\theta_1, \theta_2, \ldots, \theta_m)$ so that the modeled data points $I_k(\theta)$ are close to the corresponding observed data points $\tilde{I}_k$, in an appropriate least squares sense. In order to do this, it is necessary to have reasonable starting guesses for the parameters, and to evaluate $I_k(\theta)$ for various parameter sets $\theta$ to some appropriate level of accuracy, in an efficient manner.

The main body of this report consists of three sections. Section 2 is concerned with the problem of efficient and accurate computer evaluation of (1.1) given $w_k(v)$ in tabular form, and trial values of $\theta$. This problem is nontrivial, because, among other reasons, the operation must be repeatedly performed many times.

In Section 2 we consider the class of quadrature formulae which would be exact if $f(v;\theta)$ were linear in the components of $v$. (The quadrature coefficients then depend on $w_k$ and are pre-calculated). A fairly sharp upper bound for the quadratures error is given, which depends (for given $w_k(v)$) on the number and location of the quadrature points and the largest possible value of the mixed second partial derivatives of $f(v;\theta)$ with respect to the components of $v$.

If the instrument response windows are much longer in the $\beta$ direction than in either the $v$ or $\alpha$ direction (which is apparently the case), it makes sense to consider a linear array of quadrature points in this direction only.

For this case a feasible procedure is given whereby, for any fixed number $n$, the optimal set of quadrature points may be found. The optimal set of points is that set for which the error bound of the quadratures error is the smallest possible, assuming that a linear array is adequate. Upon finding the optimal set for each $n$ under consideration, the corresponding error bound may be determined to see if it is within the system accuracy constraints. Then the set with smallest $n$ meeting the system constraints is selected.

The adequacy of the linear array assumption may be checked by inspection of the final optimal set as determined above. A two dimensional procedure is described, for use if the one dimensional array is not adequate.

In a simple analytic example the number of quadrature points required to meet a fixed error bound was found to be reduced by about 25-30% by use of the procedure given, as compared to equally spaced points.

Although the procedure given may appear to require a large amount of effort, the more time consuming steps (involved with organization and numerical integration of the calibration data), will have to be done for any accurate numerical integration procedure.

Section 3 briefly describes a least-squares procedure for estimating the Helium fraction, which probably has the advantage of being more stable than letting the Helium fraction be a free parameter in the general non-linear least squares parameter estimation program.

Section 4 gives an algorithm for linear estimates of the plasma parameters. A draft of this section was delivered informally in August, 1970.

Section 5 is conclusions, and Section 6 contains three appendices.

## SECTION 2.

## OPTIMIZATION OF THE NUMERICAL QUADRATURE

### 2.1. General Considerations in the Optimization of the Numerical Quadrature, Introduction.

Let $f(v,\theta)$ be the particle velocity vector distribution with parameters $\theta$, $\theta = (\theta_1,\theta_2,\ldots,\theta_m)$. Let $w_k(v)$ be the instrument response to a unit number density cold beam with velocity vector $\bar{v}$ at the $k^{th}$ choice of collector, energy step and instrument position relative to the solar-oriented ecliptic coordinate system. In the discussion below we will suppress the subscript $k$. Thus $w(v) = w_k(v)$ for fixed $k$. $w(\bar{v})$ is determined in the laboratory, for selected values of $v$, and the functional form of $f(v,\theta)$, as well as bounds on the possible values of $\theta$ are known. The problem considered here is to develop an efficient quadrature procedure for evaluating numerically

$$I(\theta) = \iiint f(v,\theta)w(v)dv \quad . \tag{2.1.1}$$

It is highly desirable to do this with as few quadrature points as possible, since, $I(\theta)$ must be evaluated (for each k) for many different values of $\theta$, each time the plasma parameters are estimated iteratively by non-linear least squares.

Let

$$\hat{I}(\theta) = \sum_{\nu=1}^{n} f(x^{\nu},\theta) \iiint_{R_\nu} w(v)dv \tag{2.1.2}$$

where $n$ is the number of quadrature points, $R_1, R_2, \ldots, R_n$ are $n$ disjoint regions in Euclidean 3 space to be determined, whose union is $S$, $S$ being the region for which $w(v) > 0$, and $x^\nu$, $\nu = 1,2,\ldots,n$ are $n$ vectors to be determined, $x^\nu \in R_\nu$. Equation (2.1.2) is known as the quadrature formula. $\iiint_{R_\nu} w(v)dv$ is calculated and stored in advance, so only given linear combinations of $f(x^\nu,\theta)$, for $\nu = 1,2,\ldots,n$ are calculated during the iterative estimation of $\theta$. Then

$$I(\theta) - \hat{I}(\theta) = \sum_{\nu=1}^{n} \iiint_{R_\nu} w(v)[f(v,\theta)-f(x^\nu,\theta)]dv \quad . \tag{2.1.3}$$

By expanding $f(v,\theta)$ is a Taylor series about $x^\nu$, and letting $v = (v_1,v_2,v_3)$, $x^\nu = (x_1^\nu,x_2^\nu,x_3^\nu)$, we have

$$f(v,\theta)-f(x^\nu,\theta) = \sum_{j=1}^{3} \frac{\partial f(x^\nu,\theta)}{\partial x_j^\nu}(v_j-x_j^\nu) + \frac{1}{2!}\sum_i \sum_j \left.\frac{\partial^2 f(v,\theta)}{\partial v_i \partial v_j}\right|_{v=v_*} (v_i-x_i^\nu)(v_j-x_j^\nu) \tag{2.1.4}$$

where $v_*$ is some point between $v$ and $x^\nu$, depending on $v$.

Thus

$$I(\theta) - \hat{I}(\theta) = \left\{ \sum_{\nu=1}^{n} \sum_{j=1}^{3} \frac{\partial f(x^{\nu},\theta)}{\partial x_j^{\nu}} \iiint_{R_\nu} w(v)(v_j - x_j^{\nu})dv \right\}$$

$$+ \sum_{\nu=1}^{n} \frac{1}{2!} \iiint_{R_\nu} w(v) \sum_{i=1}^{3} \sum_{j=1}^{3} \left. \frac{\partial^2 f(v,\theta)}{\partial v_i \partial v_j} \right|_{v=v_*} (v_i - x_i^{\nu})(v_j - x_j^{\nu})dv \ . \tag{2.1.5}$$

If $x_j^{\nu}$ is always chosen so that

$$x_j^{\nu} = \frac{\iiint_{R_\nu} v_j w(v)dv}{\iiint_{R_\nu} w(v)dv} \quad , \quad j = 1,2,3 \ , \tag{2.1.6}$$

then the first term in (2.1.5) is identically 0. In Appendix A we show that, for a Maxwellian distribution

$$\max_{v,\ \theta,i,j} \left| \frac{\partial^2 f(v,\theta)}{\partial v_i \partial v_j} \right| = M \tag{2.1.7}$$

where

$$M = \frac{N}{(2\pi)^{3/2}\sqrt{\lambda_1\lambda_2\lambda_3}} \quad \frac{1}{\lambda_{min}} \tag{2.1.8}$$

where $N$ is the number density, $\lambda_i = \frac{kT_i}{m}$, where $k$ is Boltzman's constant, m is the particle mass, and $T_i$ is temperature along the direction of the eigenvector of the pressure tensor corresponding to

the eigenvalue $\lambda_i$. $\sqrt{\lambda_i}$ is in units of velocity. If $f(v,\theta)$ is the sum of two Maxwellian distributions as in (3.2.5) then (2.1.8) holds with N replaced by $N_p+2N_\alpha$, $N_p$ and $N_\alpha$ being the proton and $\alpha$-particle number densities, respectively. Also, letting $\|x\|^2 = x_1^2+x_2^2+x_3^2$,

$$\sum_{i=1}^{3}\sum_{j=1}^{3}(v_i-x_i^\nu)(v_j-x_j^\nu) \leq 3\sum_{i=1}^{3}(v_i-x_i^\nu)^2 = 3\|v-x^\nu\|^2$$

$$\leq 3 \max_{\xi,\eta\in R_\nu} \|\xi-\eta\|^2 \quad , \quad v \in R_\nu \tag{2.1.9}$$

$\max_{\xi,\eta\in R_\nu} \|\xi-\eta\|$ is the maximum dimension of the region $R_\nu$. Therefore, if $x_j^\nu$ is chosen as in (2.1.6), then

$$|I(\theta)-\hat{I}(\theta)| \leq \frac{3}{2}M \sum_{\nu=1}^{n} \max_{\xi,\eta\in R_\nu} \|\xi-\eta\|^2 \iiint_{R_\nu} w(v)dv \quad . \tag{2.1.10}$$

The main idea of the preceeding discussion (Eqns. (2.1.3)-(2.1.6) and (2.1.9)-(2.1.10)) has been adapted from a memo of Mr. John Day, of Informatics.

Assuming that $w(v)$ has units of current per unit number density, then $I(\theta) - \hat{I}(\theta)$ has units of current, $M$ has units of (number density $\times$ velocity$^{-5}$), $\max_{\xi,\eta\in R_\nu} \|\xi-\eta\|^2$ has units of velocity$^2$, and $\iiint_{R_\nu} w(v)dv$ has units of (current $\times$ number density$^{-1}$ $\times$ velocity$^3$).

We now proceed under the assumption that accuracy standards on the quadrature can be established based on 1) the requirements for accuracy in the non-linear least squares program 2) the accuracy of the calibration data $w(v)$ and 3) other system errors (including digitization, timing uncertainties and the inability to accurately recover the signal current at the output of the collectors). Thus, we wish to find $n$, and $\{R_\nu\}_{\nu=1}^{n}$ so that $n$ is as small as possible subject to the constraint

$$|I(\theta)-\hat{I}(\theta)| \leq \frac{3}{2} M \sum_{\nu=1}^{n} \max_{\xi,\eta\in R_\nu} ||\xi-\eta||^2 \iiint_{R_\nu} w(v)dv \leq C_1 \qquad (2.1.11)$$

where $C_1$ is given (in units of current).

Thus, we must find the smallest feasible and practical $n$, and corresponding sets $\{R_\nu\}_{\nu=1}^{n}$, $\{x^\nu\}_{\nu=1}^{n}$ for which

$$\sum_{\nu=1}^{n} \max_{\xi,\eta\in R_\nu} ||\xi-\eta||^2 \iiint_{R_\nu} w(v)dv \leq C_2 = \frac{2}{3}\frac{1}{M} C_1 \quad . \qquad (2.1.12)$$

The remainder of this Section is divided into four subsections. In Section 2.2 we derive some theoretical lower bounds for

$$\sum_{\nu=1}^{n} \max_{\xi,\eta\in R_\nu} ||\xi-\eta||^2 \iiint_{R_\nu} w(v)dv \quad . \qquad (2.1.13)$$

The purpose of this is twofold. 1. The results can be used to tell us

whether it is worthwhile to attempt to improve a given choice of $\{R_\nu\}_{\nu=1}^{n}$, that is, how close is a given choice to the best obtainable. 2. The conditions under which the theoretical lower bound is attained give us some qualitative criteria for a good set $\{R_\nu\}_{\nu=1}^{n}$ for given n. In Section 2.3 we discuss qualitatively some of the calibration data available during the period of this study. Based on the criteria developed in Section 2.2, it appears that a satisfactory solution may well be obtained by exploiting the fact that the instrument response windows are much narrower in the radial (increasing $\frac{E}{q}$) and azimuthal ($\alpha$) directions than the elevation ($\beta$) direction.

In Section 2.4, the results of Section 2.3 are used to formulate the problem of choosing the $\{R_\nu\}_{\nu=1}^{n}$ as a much simpler problem, namely as a problem in determining boundaries in one dimension, instead of three. For this simpler problem we given an algorithm for obtaining starting guesses for the boundaries of the regions $\{R_\nu\}_{\nu=1}^{n}$ which minimize

$$\sum_{\nu=1}^{n} \max_{\xi,\eta\in R_\nu} ||\xi-\eta||^2 \iiint_{R_\nu} w(v)dv \qquad (2.1.13)$$

for any given n. The calibration data is used to define w(v) here. The use of Newton's method to iteratively improve the choice of boundaries to minimize (2.1.13), and the convergence properties of

this method, are described. For each candidate value of $n$, then, the best or near best set of boundaries may be found by the method described. Then the smallest $n$ for which the inequality (2.1.12) holds may then be selected. Section 2.5 discusses a check for determining whether the one-dimensional solution is adequate. A two dimensional procedure is discussed in the (unlikely) case that it is not. In Section 2.6 a simple example is discussed in which the roughly 30% fewer quadrature points are required for the best choice of points as compared to equally spaced points, for the same accuracy.

## 2.2. Theoretical Lower Bounds for the Quadrature Error and Properties of a Good Choice of Regions

By use of the Hölder and Jensen inequalities we first obtain a theoretical lower bound on

$$\sum_{\nu=1}^{n} \max_{\xi,\eta\in R_\nu} \|\xi-\eta\|^2 \iiint_{R_\nu} w(v)dv \qquad (2.1.13)$$

over all possible choices of regions $\{R_\nu\}$ whose union covers $S$. By examining the conditions under which this theoretical lower bound is attained, we obtain clues as to the properties of a good choice of regions.

The volume $V$ of a sphere in 3 dimensional Euclidean space is given by

$$V = \frac{\pi}{6} d^3 \ , \qquad (2.2.1)$$

where $d$ is the diameter. Since a sphere is the geometric figure which maximizes the ratio of the volume to the longest dimension, we always have

$$\max_{\xi,\eta\in R_\nu} ||\xi-\eta||^2 \geq C \left(\iiint_{R_\nu} dv\right)^{2/3} \tag{2.2.2}$$

where $C = C_3 = \left(\frac{6}{\pi}\right)^{2/3} \tilde{=} 1.54$ and equality is obtained if and only if $R_\nu$ is a sphere. In general, S, the region over which $w(v) > 0$, cannot be partitioned into spheres. If S is partitioned by, say plane surfaces only, then we will have $C = C_4 = 2^2 = 4$, obtained for $R_\nu$ a cube, since then $V^{1/3}$ = length of a side = 2 × longest dimension.

Therefore, provided only planes are used to partition S, then

$$\sum_{\nu=1}^{n} \max_{\xi,\eta\in R_\nu} ||\xi-\eta||^2 \iiint_{R_\nu} w(v)dv \geq C_4 \sum_{\nu=1}^{n} \left[\iiint_{R_\nu} dv\right]^{2/3} \left[\iiint_{R_\nu} w(v)dv\right] \tag{2.2.3}$$

with equality holding if and only if $\{R_\nu\}$ are all cubes.

The famous Hölder inequality says, for any $\alpha$, $\beta$ positive numbers with $\alpha+\beta = 1$, and $a(v)$, $b(v)$ positive functions,

$$\iiint_{R_\nu} a^\alpha(v)b^\beta(v)dv \leq \left[\iiint_{R_\nu} a(v)dv\right]^\alpha \left[\iiint_{R_\nu} b(v)dv\right]^\beta \tag{2.2.4}$$

with equality holding if and only if $a(v)$ is a constant times $b(v)$. Letting $\alpha = \frac{2}{5}$ , $\beta = \frac{3}{5}$ , $a(v) \equiv 1$, $b(v) = w(v)$, we have

$$\iiint_{R_\nu} w^{3/5}(v)dv \leq \left[\iiint_{R_\nu} dv\right]^{2/5} \left[\iiint_{R_\nu} w(v)dv\right]^{3/5} , \qquad (2.2.5)$$

and, taking the 5/3 power of both sides, we have

$$\left[\iiint_{R_\nu} w^{3/5}(v)dv\right]^{5/3} \leq \left[\iiint_{R_\nu} dv\right]^{2/3} \left[\iiint_{R_\nu} w(v)dv\right] \qquad (2.2.6)$$

and

$$C_4 \sum_{\nu=1}^{n} \left[\iiint_{R_\nu} dv\right]^{2/3} \left[\iiint_{R_\nu} w(v)dv\right] \geq C_4 \sum_{\nu=1}^{n} \left[\iiint_{R_\nu} w^{3/5}(v)dv\right]^{5/3} \qquad (2.2.7)$$

with equality holding if and only if $w(v)$ is constant on each $R_\nu$.

By Jensen's Inequality (see Appendix B), we have

$$C_4 \sum_{\nu=1}^{n} \left[\iiint_{R_\nu} w^{3/5}(v)dv\right]^{5/3} \geq C_4 n \left[\frac{1}{n} \sum_{\nu=1}^{n} \iiint_{R_\nu} w^{3/5}(v)dv\right]^{5/3}$$

$$= \frac{C_4}{n^{2/3}} \left[\iiint_{S} w^{3/5}(v)dv\right]^{5/3} \qquad (2.2.8)$$

with equality holding if and only if

$$\iiint_{R_\nu} w^{3/5}(v)dv = \iiint_{R_\mu} w^{3/5}(v)dv \quad , \quad \text{all } \mu,\nu \ . \qquad (2.2.9)$$

In summary, for any partition of $S$ into $n$ disjoint regions $\{R_\nu\}_{\nu=1}^{n}$ whose union is $S$, a universal lower bound for (2.1.13) is given by

$$\sum_{\nu=1}^{n} \max_{\xi,\eta\in R_\nu} \|\xi-\eta\|^2 \iiint_{R_\nu} w(v)dv \geq \frac{C_4}{n^{2/3}}\left[\iiint_S w^{3/5}(v)dv\right]^{5/3} . \quad (2.2.10)$$

The lower bound is attained if and only if equality obtains in (2.2.2), (2.2.7) and (2.2.8)) which means (restricting the partitions to planes, to simplify the discussion).

i) All the $R_\nu$ are cubes (that is, the ratio of volume to (diameter)$^3$ is maximized

ii) $w(v)$ is constant on each $R_\nu$

iii) The volume of $R_\nu$ is inversely proportional to $w^{3/5}(x^\nu)$, $x^\nu \in R_\nu$ .

This lower bound cannot be obtained for arbitrary $w(v)$ since, for example i) and ii) require $w(v)$ to be constant on cubes. However, from the above we may make the following semi-quantitative statements about properties of a good partition.

i) The ratio of the longest to the shortest dimension of each $R_\nu$ should not be too large

ii) The regions should be chosen so that $w(v)$ does not vary much for $v \in R_\nu$ .

iii) The volume of the regions should be small where $w(v)$ is large, and conversely.

## 2.3 Analysis of the Calibration Data and Simplification of The Problem

The following discussion assumes, for concreteness, that the calibration coordinate system is a spherical coordinate system. In a spherical system a cold beam with rectangular coordinates $(v_1,v_2,v_3)$ has velocity $r = (v_1^2+v_2^2+v_3^2)^{1/2}$, and angles of incidence $\alpha$ and $\beta$ where

$$\begin{aligned} v_1 &= r \cos\beta \sin\alpha \\ v_2 &= r \sin\beta \\ v_3 &= r \cos\beta \cos\alpha \end{aligned} \qquad (2.3.1)$$

See Figure 2.1. In what follows the volume element $dv_1\, dv_2\, dv_3$ is replaced by the spherical volume element $r^2 \cos\beta\, dr d\beta d\alpha$. If the calibration coordinate system is not exactly spherical, the appropriate volume element should be used, but the remainder of the discussion below is unaffected.

Let $w(v_1,v_2,v_3)$ be the response of the instrument to a cold beam of protons of unit number density and coordinates $v_1,v_2,v_3$. $w(v_1,v_2,v_3)$ is actually measured by 1) Fixing $r$ and $\beta$ and

varying $\alpha$. 2) Fixing r and $\alpha$ and varying $\beta$. 3) Choosing a new r and repeating 1) and 2). Thus, it will be convenient to perform some calculations involving calibration data in the calibration coordinate system.

Figures 2.2 and 2.3 reproduce some calibration curves and a plot which were available while this study was being performed. Complete labels and scale factors were not all provided and the missing information is omitted. Some labels have been added according to the coordinate system assumed in Figure 2.1.

Figure 2.4 shows a hypothetical calibration curve as it might appear if the incidence angles $\alpha$, $\beta$ are kept fixed and the calibration bean velocity is varied. Based on discussions with ARC personnel, it is assumed that the resolution of the instrument in the (E/q) direction, i.e. in the direction of increasing beam velocity, is very narrow compared to the resolution in the direction of changing $\alpha$ or $\beta$.

That is, the width of the curve in Figure 2.4 is very narrow compared to that of Figure 2.2a, when both are visualized in a common rectangular system.

Figure 2.5 depicts schematically $\alpha$ and $\beta$ calibration curves transformed to a rectangular system, for fixed r. Inspection of Figures 2.3 and 2.4 and their visualization in a common rectangular coordinate system reveals that the region S in a rectangular system for which w is not zero is shaped roughly like a possibly flattened hot dog.

A cross section of this hot dog shaped region, for fixed $r$, is the shaded region of Figure 2.5. The full hot dog shaped region $S$ is depicted schematically in Figure 2.6. This is the region that must be partitioned. Due to the highly elongated shape of this region, it is consistent with the criteria for a good partition at the end of Section 1. to consider partitions perpendicular to the long axis of $S$. There is considerable benefit to being able to describe the partition simply in the calibration coordinate system. To this end, consider slicing (i.e. partitioning) the hot dog $S$ with cones of constant $\beta$. If this is done, then a Region $R_\nu$ consists of all points whose polar coordinates $(r, \alpha,\beta)$ satisfy

$$\begin{aligned} &(r, \alpha,\beta) \in S' \\ &\beta_\nu \leq \beta < \beta_{\nu+1} \end{aligned} \tag{2.3.2}$$

where the cones determined by $\beta = \beta_\nu$ and $\beta = \beta_{\nu+1}$ are two boundaries of $R_\nu$. Figure 2.7 shows a cross section of the region $S$ in the $r, \beta$ plane, for $\alpha = 0$, and a cross section of $R_\nu$ with boundaries $\beta = \beta_\nu$ and $\beta = \beta_{\nu+1}$.

Then, if we abuse notation by letting $w(r,\alpha,\beta)$ be the instrument response to a beam with spherical coordinates $r$, $\alpha$, $\beta$, then

$$\iiint_{R_\nu} w(v_1,v_2,v_3)dv_1dv_2dv_3 = \int_{\beta_\nu}^{\beta_{\nu+1}} \cos\beta d\beta \int_{\alpha=0}^{2\pi} d\alpha \int_{r=0}^{\infty} w(r,\alpha,\beta)r^2dr \tag{2.3.2}$$

Of course the limits $r = 0$, $r = \infty$ and $\alpha = 0$, $\alpha = 2\pi$ could be replaced by the extreme values of $r$ and $\alpha$ inside $S$.

Define

$$h(\beta) = \cos\beta \int_{\alpha=0}^{2\pi} d\alpha \int_{r=0}^{\infty} w(r,\alpha,\beta) r^2 dr \quad . \tag{2.3.4}$$

We may rewrite (2.3.3) as

$$\iiint_{R_\nu} w(v_1,v_2,v_3)dv_1dv_2dv_3 = \int_{\beta_\nu}^{\beta_{\nu+1}} h(\beta)d\beta \quad . \tag{2.3.5}$$

We next suppose that the longest dimension of $R_\nu$ will always be in the $\beta$ direction. If $S$ is to be partitioned into, say 8 or 9 regions then this is reasonable since the hot dog $S$ is around say 8 or 9 times as long as it is thick, loosely speaking. In this case, the maximum dimension of $R_\nu$ is given by

$$\max_{\xi,\eta\in R_\nu} ||\xi-\eta|| = r_*|\beta_{\nu+1}-\beta_\nu| \tag{2.3.6}$$

where $r_*$ is some intermediate value of $r$ in $S$. See Figure 2.7. With the restrictions that a) $S$ is to be partitioned by cones of constant $\beta$ and b) the longest dimension of $R_\nu$ is in the $\beta$ direction, we may write

$$\sum_{\nu=1}^{m} \max_{\xi,\nu\in R_\nu} ||\xi-\eta||^2 \iiint_{R_\nu} w(v_1,v_2,v_3)dv_1dv_2dv_3 \leq$$

$$C_4(r_{**})^2 \sum_{\nu=1}^{n} |\beta_{\nu+1}-\beta_\nu|^2 \int_{\beta_\nu}^{\beta_{\nu+1}} h(\beta)d\beta \qquad (2.3.7)$$

where $r_{**}$ is some intermediate value of $r$ inside $S$, and where $\beta_1$ and $\beta_{n+1}$ are the extreme $\beta$ values for points in $S$ (see Figure 2.7). $\beta$ is in radians in (2.3.7). If $h(\beta)$ and $n$ are given, it is possible to give an algorithm for choosing $\beta_2,\beta_3,\ldots,\beta_n$ to minimize

$$\sum_{\nu=1}^{n} |\beta_{\nu+1}-\beta_\nu|^2 \int_{\beta_\nu}^{\beta_{\nu+1}} h(\beta)d\beta \quad . \qquad (2.3.8)$$

We do this in Section 2.4. To conclude this section we discuss the determination of $h(\beta)$ from calibration data.

Let

$$\psi(\alpha,\beta) = \int_{r=0}^{\infty} w(r,\alpha,\beta)r^2dr \quad . \qquad (2.3.9)$$

Then

$$h(\beta) = \cos\beta \int_{\alpha=0}^{2\pi} \psi(\alpha,\beta)d\alpha \quad . \qquad (2.3.10)$$

$\psi(\alpha,\beta)$ is the area under the curve $r^2w(r,\alpha,\beta)$, as a function of $r$, where the curve $w(r,\alpha,\beta)$ as a function of $r$ is shown in Figure 2.4.

If the calibration points are taken at a sufficiently fine grid, $\beta = \beta^{(1)},\beta^{(2)},\ldots,\beta^{(n_\beta)}$, $\alpha = \alpha^{(1)},\alpha^{(2)},\ldots,\alpha^{(n_\alpha)}$, $r = r^{(1)},r^{(2)},\ldots,r^{(n_r)}$, then

$$h(\beta^{(i)}) \approx \cos\beta^{(i)} \sum_{j=1}^{n_\alpha} \sum_{k=1}^{n_r} w\left(r^{(k)},\alpha^{(j)},\beta^{(i)}\right)\left(r^{(k)}\right)^2 \times \left(\frac{\alpha^{(j+1)}-\alpha^{(j-1)}}{2}\right)\left(\frac{r^{(k+1)}-r^{(k-1)}}{2}\right) \tag{2.3.11}$$

where $w\left(r^{(k)},\alpha^{(j)},\beta^{(i)}\right)$ are measured values of $w$, and $\alpha^{(0)}$, $\alpha^{(n_\alpha+1)}$, $r^{(0)}$, and $r^{(n_r+1)}$ are suitably chosen.

We may write

$$h(\beta^{(i)}) \approx \cos\beta^{(i)} \sum_{j=1}^{n_\alpha} \frac{(\alpha^{(j+1)}-\alpha^{(j-1)})}{2} \tilde{\psi}\,(\alpha^{(j)},\beta^{(i)}) \tag{2.3.12}$$

where

$$\tilde{\psi}(\alpha^{(j)},\beta^{(i)}) = \sum_{k=1}^{n_r} w\left(r^{(k)},\alpha^{(j)},\beta^{(i)}\right)\left(r^{(k)}\right)^2\left(\frac{r^{(k+1)}-r^{(k-1)}}{2}\right)$$

$$\approx \int_{r=0}^{\infty} w\left(r,\alpha^{(j)},\beta^{(i)}\right) r^2 dr \quad . \tag{2.3.13}$$

If the calibration points in the $r$ direction are sparse, as in Figure 2.4, then the approximation in (2.3.13) will not be good, and care must be taken to get sufficiently accurate values of $\tilde{\psi}(\alpha^{(j)},\beta^{(i)})$.

Now, suppose we have determined $h(\beta)$ for $\beta = \beta^{(1)},\beta^{(2)},\ldots,\beta^{(n_\beta)}$ where $\beta^{(i+1)} - \beta^{(i)}$ is much smaller than the difference between two possible region boundaries $\beta_{\nu+1} - \beta_\nu$. Say $\beta^{(i+1)} - \beta^{(i)} \simeq 1°$. We will then proceed below as though $h(\beta) = 0$ for $\beta < \beta_1$, and $\beta > \beta_{n+1}$ and is known continuously for $\beta_1 \leq \beta \leq \beta_{n+1}$. The next section gives an algorithm for minimizing (2.3.8).

## 2.4 Choosing an Optimal Set of $\{\beta_2,\beta_3,\ldots,\beta_n\}$

The problem now is to choose $\beta_2,\beta_3,\ldots,\beta_n$ satisfying $\beta_1 < \beta_2 < \ldots < \beta_n < \beta_{n+1}$ to minimize $f(\beta_2,\beta_3,\ldots,\beta_n)$ given by

$$f(\beta_2,\beta_3,\ldots,\beta_n) = \sum_{\nu=1}^{n} (\beta_{\nu+1}-\beta_\nu)^2 \int_{\beta_\nu}^{\beta_{\nu+1}} h(\beta)d\beta \quad . \qquad (2.4.1)$$

By the Hölder inequality of (2.2.4) with $\alpha = \frac{2}{3}$, $\beta = \frac{1}{3}$ we have

$$\left( \int_{\beta_\nu}^{\beta_{\nu+1}} d\beta \right)^{\frac{2}{3}} \left( \int_{\beta_\nu}^{\beta_{\nu+1}} h(\beta)d\beta \right)^{\frac{1}{3}} \geq \int_{\beta_\nu}^{\beta_{\nu+1}} [h(\beta)]^{\frac{1}{3}} d\beta \quad . \qquad (2.4.2)$$

Hence, upon cubing both sides of (2.4.2) and summing, we have

$$\sum_{\nu=1}^{n} (\beta_{\nu+1}-\beta_{\nu}) \int_{\beta_\nu}^{\beta_{\nu+1}} h(\beta)d\beta \geq \sum_{\nu=1}^{n}\left( \int_{\beta_\nu}^{\beta_{\nu+1}} [h(\beta)]^{\frac{1}{3}} d\beta \right)^3 . \quad (2.4.3)$$

Equality holds in (2.4.3) if and only if $h(\beta)$ is a constant for $\beta_\nu \leq \beta \leq \beta_{\nu+1}$ .

By Jensen's inequality, we have

$$\sum_{\nu=1}^{n}\left( \int_{\beta_\nu}^{\beta_{\nu+1}} [h(\beta)]^{\frac{1}{3}} d\beta \right)^3 \geq n\left[ \frac{1}{n}\sum_{\nu=1}^{n} \int_{\beta_\nu}^{\beta_{\nu+1}} [h(\beta)]^{\frac{1}{3}} d\beta \right]^3 = \frac{1}{n^2}\left[ \int_{\beta_\nu}^{\beta_{\nu+1}} [h(\beta)]^{\frac{1}{3}} d\beta \right]^3 \quad (2.4.4)$$

with equality holding if and only if the $\{\beta_\nu\}$ are chosen so that

$$\int_{\beta_\nu}^{\beta_{\nu+1}} [h(\beta)]^{\frac{1}{3}} d\beta = \frac{1}{n} \int_{\beta_1}^{\beta_{n+1}} [h(\beta)]^{\frac{1}{3}} d\beta \quad . \quad (2.4.5)$$

The (unique) values $\beta_2^*,\beta_3^*,\ldots,\beta_n^*$ for which (2.4.5) is satisfied may be found graphically by plotting

$$H(\beta) = \int_{\beta_1}^{\beta} [h(\beta)]^{\frac{1}{3}} d\beta \Big/ \int_{\beta_1}^{\beta_{n+1}} [h(\beta)]^{\frac{1}{3}} d\beta \quad (2.4.6)$$

and graphically finding $\beta_\nu^*$ which satisfies

$$H(\beta_\nu^*) = \frac{\nu-1}{n} \quad , \quad \nu = 2,3,\ldots,n \quad . \tag{2.4.7}$$

This graphical procedure is illustrated in Figure 2.8.

Now the set $\beta_2^*,\beta_3^*, \ldots, \beta_n^*$ found this way does not, in general, minimize $f(\beta_2,\ldots,\beta_n)$ since equality does not, in general hold in (2.4.3). However, it is shown in Appendix C that

$$\begin{aligned} \sum_{\nu=1}^{n} (\beta_{\nu+1}^*-\beta_\nu^*)^2 \int_{\beta_\nu^*}^{\beta_{\nu+1}^*} h(\beta)d\beta - \frac{1}{n^2}\left[\int_{\beta_1}^{\beta_{n+1}} [h(\beta)]^{\frac{1}{3}}\, d\beta\right]^3 \\ \leq \sum_{\nu=1}^{n-1} |\beta_{\nu+1}^*-\beta_\nu^*|^4 \max_{\theta\in(\beta_\nu^*,\beta_{\nu+1}^*)} h'(\theta) \end{aligned} \tag{2.4.8}$$

where, according to (2.4.4) $\frac{1}{n^2}\left[\int_{\beta_1}^{\beta_{n+1}} [h(\beta)]^{\frac{1}{3}}\, d\beta\right]^3$ is an absolute lower bound for $f(\beta_2,\beta_3,\ldots,\beta_n)$. For the derivative $h'$ not too large, and $|\beta_{\nu+1}^*-\beta_\nu^*|^4$ small (remember $\beta$ is in radians here), (2.4.8) shows that the chosen $\beta_2^*,\beta_3^*,\ldots,\beta_n^*$, found by solving (2.4.7) will be close to the best possible set. The next step is to calculate $f(\beta_2^*,\ldots,\beta_n^*)$ and determine if

$$\frac{3}{2} M \times C_4(r_{**})^2 f(\beta_2^*,\ldots,\beta_n^*) \leq C_1 \quad . \tag{2.4.9}$$

(Recall Equations (2.1.11) and (2.3.7)). If not, $n$ may be increased,

or a second order improvement in the choice of the $\{\beta_\nu\}$ attempted. Given the set $(\beta_2^*,\ldots,\beta_n^*)$ of starting values determined as above, various iterative techniques can be used to minimize $f(\beta_2,\ldots,\beta_n)$ numerically. Most likely an adaptation of the Marquardt algorithm in use in the Plasma Probe non-linear least-squares estimation program can be made to do the job. At this level, the improvement possible will, in general, be only second order. For completeness, we describe a relatively simple procedure for improving the set $(\beta_2^*,\beta_3^*,\ldots,\beta_n^*)$. It is Newton's method in n-1 dimensions. It will be be convenient to use vector notation to discuss Newton's method. Let $\vec{\beta} = (\beta_2,\ldots,\beta_n)$, $f(\vec{\beta}) = f(\beta_2,\ldots,\beta_n)$ given by (2.4.1) and let

$$g(\vec{\beta}) = \begin{pmatrix} \frac{\partial f(\vec{\beta})}{\partial \beta_2} \\ \frac{\partial f(\vec{\beta})}{\partial \beta_3} \\ \vdots \\ \frac{\partial f(\vec{\beta})}{\partial \beta_n} \end{pmatrix} \qquad (2.4.10)$$

$$A(\vec{\beta}) = \begin{pmatrix} \frac{\partial^2 f(\vec{\beta})}{\partial \beta_2^2} & \cdots & \frac{\partial^2 f(\vec{\beta})}{\partial \beta_2 \partial \beta_n} \\ \vdots & \frac{\partial^2 f(\vec{\beta})}{\partial \beta_3^2} & \vdots \\ \frac{\partial^2 f(\vec{\beta})}{\partial \beta_n \partial \beta_2} & & \frac{\partial^2 f(\vec{\beta})}{\partial \beta_n^2} \end{pmatrix} \qquad (2.4.11)$$

We have

$$\frac{\partial f(\vec{\beta})}{\partial \beta_i} = 2(\beta_i - \beta_{i-1}) \int_{\beta_{i-1}}^{\beta_i} h(\beta)d\beta + (\beta_i - \beta_{i-1})^2 h(\beta_i) \qquad (2.4.12)$$

$$- \left[ 2(\beta_{i+1} - \beta_i) \int_{\beta_i}^{\beta_{i+1}} h(\beta)d\beta + (\beta_{i+1} - \beta_i)^2 h(\beta_i) \right]$$

$$i = 2,3,\ldots,n$$

$$\frac{\partial^2 f}{\partial \beta_i^2} = 4(\beta_{i+1} - \beta_{i-1})h(\beta_i) + 2 \int_{\beta_{i-1}}^{\beta_{i+1}} h(\beta)d\beta \qquad (2.4.13)$$

$$+ \quad h'(\beta_i) \left[ (\beta_i - \beta_{i-1})^2 - (\beta_{i+1} - \beta_i)^2 \right]$$

$$\frac{\partial^2 f}{\partial\beta_i \partial\beta_{i+1}} = \frac{\partial^2 f}{\partial\beta_{i+1}\partial\beta_i} = -2\left[(\beta_{i+1}-\beta_i)(h(\beta_{i+1})+h(\beta_i)) + \int_{\beta_i}^{\beta_{i+1}} h(\beta)d\beta\right]$$

$$i = 2,3,\ldots,n-1$$

$$\frac{\partial^2 f}{\partial\beta_i \partial\beta_{i+j}} = 0 \quad \text{for } j \neq -1,0,1 \qquad (2.4.14)$$

$$i = 2,3,\ldots,n-1 \ .$$

Necessary and sufficient conditions that $f(\vec{\beta}^{**})$ be a (local) minimum are that $g(\vec{\beta}^{**}) = 0$ and $A(\vec{\beta}^{**})$ be strictly positive definite. (A matrix A is strictly positive definite if $\vec{x}A\vec{x}' > 0$ for all vectors $\vec{x}$.) Here we then have

$$f(\vec{\beta}) = f(\vec{\beta}^{**}) + (\vec{\beta}-\vec{\beta}^{**})g(\vec{\beta}^{**}) + \frac{1}{2}(\vec{\beta}-\vec{\beta}^{**})A(\vec{\beta}^{**})(\vec{\beta}-\vec{\beta}^{**}) + \text{higher order terms} \qquad (2.4.15)$$

and, if $g(\beta^{**}) = 0$, then $f(\vec{\beta})-f(\vec{\beta}^{**}) > 0$ in the neighborhood of $\beta^{**}$. A sufficient condition that $A(\vec{\beta})$ be strictly positive definite is

$$\frac{\partial^2 f(\vec{\beta})}{\partial\beta_i^2}\ \frac{\partial^2 f(\vec{\beta})}{\partial\beta_j^2} > \left(\frac{\partial^2 f(\vec{\beta})}{\partial\beta_i \partial\beta_j}\right)^2 \quad i,j = 2,3,\ldots,n \ . \qquad (2.4.16)$$

This condition holds here if

$$h'(\beta_i)\left[(\beta_i-\beta_{i-1})^2-(\beta_{i+1}-\beta_i)^2\right] \quad i=2,3,\ldots,n \qquad (2.4.17)$$

is positive or sufficiently small negative.

If the variation in $h(\beta)$ for $\beta_{i-1} \leq \beta \leq \beta_{i+1}$ is not large compared to $h(\beta)$ for $\beta_{i-1} \leq \beta \leq \beta_{i+1}$ [1/], or, if $(\beta_{i+1}-\beta_i)^2 \approx (\beta_i-\beta_{i-1})^2$, then

$$h'(\beta_i)\left[(\beta_i-\beta_{i-1})^2 - (\beta_{i+1}-\beta_i)^2\right] \tag{2.4.18}$$

is small compared to the remainder of the contribution to $\frac{\partial^2 f}{\partial \beta_i^2}$, that is, to

$$4(\beta_{i+1}-\beta_{i-1})h(\beta_i) + 2\int_{\beta_{i-1}}^{\beta_{i+1}} h(\beta)d\beta \tag{2.4.19}$$

and can be ignored. In the computations below it may be appropriate to do this. If not, $h'(\beta_i)$ should be estimated from the calibration data, possibly by first smoothing $h(\beta)$.

To derive Newton's method expand $g(\vec{\beta})$ to the first order in a Taylor series about $\vec{\beta}^*$. Then

$$g(\vec{\beta}) \approx g(\vec{\beta}^*) + A(\vec{\beta}^*)(\vec{\beta}-\beta^*)' \quad . \tag{2.4.20}$$

[1/] Note that this is independent of the units in which $\beta$ is measured.

Then, to get $\vec{\beta}^{**}$ for which $g(\vec{\beta}^{**}) \simeq 0$, we have

$$g(\vec{\beta}^{**}) = 0 \simeq g(\vec{\beta}^{*}) + A(\vec{\beta}^{*})(\vec{\beta}^{**}-\vec{\beta}^{*})' \qquad (2.4.21)$$

and $\vec{\beta}^{**}$ is obtained from

$$\vec{\beta}^{**}-\vec{\beta}^{*} = - A^{-1}(\vec{\beta}^{*})g(\vec{\beta}^{*}) \quad . \qquad (2.4.22)$$

This procedure may be repeated with $\vec{\beta}^{**}$ as a new starting guess. If $A(\vec{\beta})$ is strictly positive definite for all $\vec{\beta}$ with $\beta_2 < \beta_3 < \ldots < \beta_n$, then $f(\vec{\beta})$ is a convex function with a unique minimum, and Newton's method is guaranteed to converge to the minimum. If, whenever $h(\beta)$ is increasing at $\beta_i$, we have $(\beta_i-\beta_{i-1})>(\beta_{i+1}-\beta_i)$ and conversely, then $A$ is strictly positive definite. This will be the usual case for the starting guess $\vec{\beta}^{*} = (\beta_2^{*},\beta_3^{*},\ldots,\beta_n^{*})$, since, loosely speaking, the method for choosing $\vec{\beta}^{*}$ selects $\beta_{i+1}^{*}-\beta_i^{*}$ inversely proportional to the average of $h^{1/3}(\beta)$ for $\beta\epsilon[\beta_i^{*},\beta_{i+1}^{*}]$. Thus we may expect that this procedure will converge rapidly to values of $\beta_2,\ldots,\beta_n$ which minimize (2.4.1).

So far, we have assumed that the longest dimension of the regions found this way is in the $\beta$ direction. If this turns out to be the case then if (2.4.9) is satisfied, then (2.1.11) will be satisfied. If $S$ is much wider in the $\alpha$ direction than $\beta_{\nu+1}^{**}-\beta_{\nu}^{**}$, where

$(\beta_2^{**},\beta_3^{*},\ldots,\beta_n^{**})$ are the solutions found above then 2 dimensional partitions should be considered. These are discussed in Section 2.5.

## 2.5 Partitions in Two Dimensions

A two dimensional partition procedure assumes that there is only one quadrature point in the $r$ direction but $n_\beta$ points in the $\beta$ direction and $n_\alpha$ in the $\alpha$ direction. Suppose a set $(\beta_2^{**},\beta_3^{**},\ldots,\beta_n^{**})$ of boundaries for the quadrature regions has been found as in Section 2.4, which meets the accuracy specifications in the sense that (2.4.9) is satisfied. Then there is no point in considering any partitioning in the $\alpha$-direction, provided that $\beta_{\nu+1}^{**} - \beta_\nu^{**}$ is greater than the angular width of $S$ in the $\alpha$ direction.

If the resulting partitions in the $\beta$ direction are half or one third of the width of $S$ in the $\alpha$ direction, then the simplest procedure is to divide all the regions $R_\nu$ in half by a contour of constant $\alpha$ down the middle. In the unlikely circumstance that the solution partitions in the $\beta$ direction are very small compared to the width of $S$ in the $\alpha$ direction, it is recommended that the problem be turned around to solve for partitions $(\alpha_2^{**},\alpha_3^{**},\ldots,\alpha_n^{**})$ in one dimension the same as was done for $\beta$.

That is, substitute $g(\alpha)$ for $h(\beta)$, where $g(\alpha)$ is given by

$$g(\alpha) = \int_{\beta=-\pi}^{\pi} \cos\beta \, d\beta \int_{r=0}^{\infty} w(r,\alpha,\beta) r^2 dr \quad , \tag{2.5.1}$$

analogous to (2.3.4), and proceed as before. Then let the final 2 dimensional partitions $R_{\mu\nu}$, $\mu = 1,2,\ldots,n'$, $\nu = 1,2,\ldots,n$ have boundaries determined by $(\alpha,\beta) \in R_{\mu,\nu}$, if $\alpha_{\mu}^{**} \leq \alpha < \alpha_{\mu+1}^{**}$, $\beta_{\nu}^{**} \leq \beta < \beta_{\nu+1}^{**}$. An (overly generous) error bound for the quadratures is given by the error bound determined individually in either the $\alpha$, or $\beta$ direction, if either direction always is the direction of the longest dimension of the regions.

It can be shown that if $\tilde{\psi}(\alpha,\beta)$ defined by

$$\tilde{\psi}(\alpha,\beta) = \psi(\alpha,\beta) \cos\beta \tag{2.5.2}$$

can be factored into the form

$$\tilde{\psi}(\alpha,\beta) = \tilde{\psi}_1(\alpha)\tilde{\psi}_2(\beta) \tag{2.5.3}$$

then the procedure for solving the problem separately in each dimension will give the partition (in 2 dimensions) minimizing (2.1.13). (Recall, for example, that the function $f(x,y) = 1$, $a_1 \leq x \leq a_2$, $b_1 \leq y \leq b_2$, and zero elsewhere, is the product of two functions $f_1(x)\, f_2(y)$, where $f_1(x) = 1$, $a_1 \leq x \leq a_2$, zero elsewhere, and

$f_2(y) = 1$, $b_1 \leq y \leq b_2$, and zero elsewhere. A bivariate normal curve suitably oriented also has this factorization property.)

## 2.6. Relative Efficiency of the Optimal Set of Quadrature Points

In this section we give a crude example to illustrate the comparison of equally spaced quadrature points in $\beta$, that is, $(\tilde{\beta}_2, \tilde{\beta}_3, \ldots, \tilde{\beta}_n)$, where

$$\frac{\tilde{\beta}_\nu - 1}{\beta_{n+1} - \beta_n} = \frac{\nu - 1}{n} \quad , \tag{2.6.1}$$

versus the $\beta_\nu^*$ chosen according to

$$\beta_\nu^* \text{ satisfies } H(\beta_\nu^*) = \frac{\nu - 1}{n} \tag{2.6.2}$$

where $H(\beta)$ is given by (2.4.6).

For simplicity, and without loss of generality, let $\beta_1 = 0$, $\beta_{n+1} = 1$. As the example, let $h(\beta) = \beta^p$. [Note that the results below will be the same for $h(\beta) = K\beta^p$ and $[0,1]$ replaced by any interval.]

Then

$$f(\tilde{\beta}_2, \tilde{\beta}_3, \ldots, \tilde{\beta}_n) \geq f(\beta_2^{**}, \beta_3^{**}, \ldots, \beta_n^{**}) \geq \frac{1}{n^2} \left[ \int_{\beta_1}^{\beta_{n+1}} [\beta^p]^{\frac{1}{3}} \, d\beta \right]^3$$

$$= \frac{1}{n^2} \frac{1}{(1 + \frac{p}{3})^3} \tag{2.6.3}$$

where $(\beta_2^{**},\beta_3^{**},\ldots,\beta_n^{**})$ are the optimal set.

From the definition (2.4.1) of $f(\beta_2,\beta_3,\ldots,\beta_n)$,

$$f(\tilde{\beta}_2,\tilde{\beta}_3,\ldots,\tilde{\beta}_n) = \frac{1}{n^2}\int_0^1 h(\beta)d\beta = \frac{1}{n^2}\,\frac{1}{(p+1)} \quad . \qquad (2.6.4)$$

For $p = 3$, the solution to (2.6.2) is

$$\beta_\nu^* = \left(\frac{\nu-1}{n}\right)^{\frac{1}{2}} \quad , \nu = 2,3,\ldots,n \qquad (2.6.5)$$

and

$$f(\beta_2^*,\ldots,\beta_n^*) = \sum_{\nu=1}^{n}\left[\left(\frac{\nu}{n}\right)^{\frac{1}{2}} - \left(\frac{\nu-1}{n}\right)^{\frac{1}{2}}\right]^2 \int_{\sqrt{\frac{\nu-1}{n}}}^{\sqrt{\frac{\nu}{n}}} \beta^3\, d\beta$$

$$= \frac{1}{4n^3}\sum_{\nu=1}^{n}\left(\nu^{\frac{1}{2}} - (\nu-1)^{\frac{1}{2}}\right)^2 (2\nu-1) \quad . \qquad (2.6.6)$$

For $p = 3$, $f(\tilde{\beta}_2,\ldots,\tilde{\beta}_n) = \frac{1}{4n^2}$ . Letting

$$\theta(n) = \frac{f(\beta_2^*,\ldots,\beta_n^*)}{f(\tilde{\beta}_2,\ldots,\tilde{\beta}_n)} \tag{2.6.7}$$

we have

$$\theta(n) = \frac{1}{n}\sum_{\nu=1}^{n} (\nu^{1/2}-(\nu-1)^{1/2})^2(2\nu-1) \tag{2.6.8}$$

$\theta(n)$ is tabulated below for $n = 4,5,\ldots,10$

| n | $\theta(n)$ |
|---|---|
| 4 | .631 |
| 5 | .605 |
| 6 | .587 |
| 7 | .575 |
| 8 | .565 |
| 9 | .558 |
| 10 | .552 |

The absolute lower bound on $f(\beta_2^{**},\ldots,\beta_n^{**})$ for $p = 3$ is $\frac{1}{4n^2} \times \frac{1}{2}$ , whereas $f(\beta_2^*,\ldots,\beta_n^*) = \frac{1}{4n^2}\theta(n)$ .

So for this case, $f(\beta_2^*,\ldots,\beta_n^*)$ is very close to the lower bound on the error, which is half that for equally spaced points. Since the error bound is inversely proportional to $n^2$, then the general conclusion, for this example, is that the number of quadrature points may be reduced, over the equally spaced case, by a factor of at least $\sqrt{\theta(n)} \approx \frac{1}{\sqrt{2}} \approx .71$.

$$dv_1\,dv_2\,dv_3 = r^2\cos\beta\,dr\,d\beta\,d\alpha$$

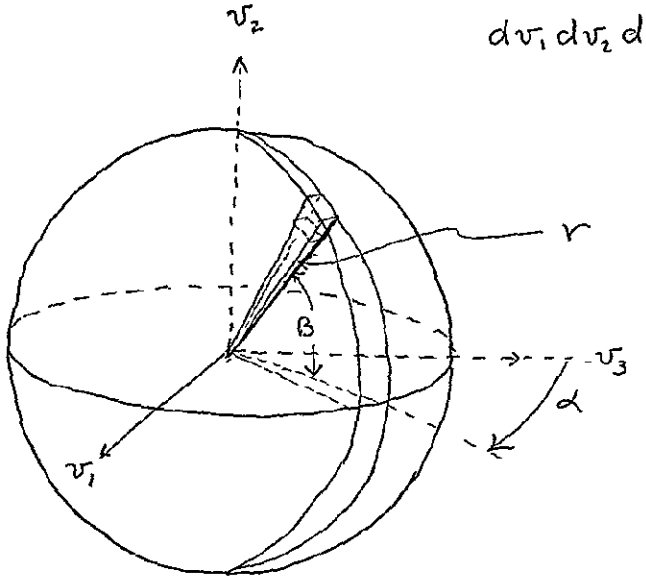


Figure 2.1

Spherical Coordinate System

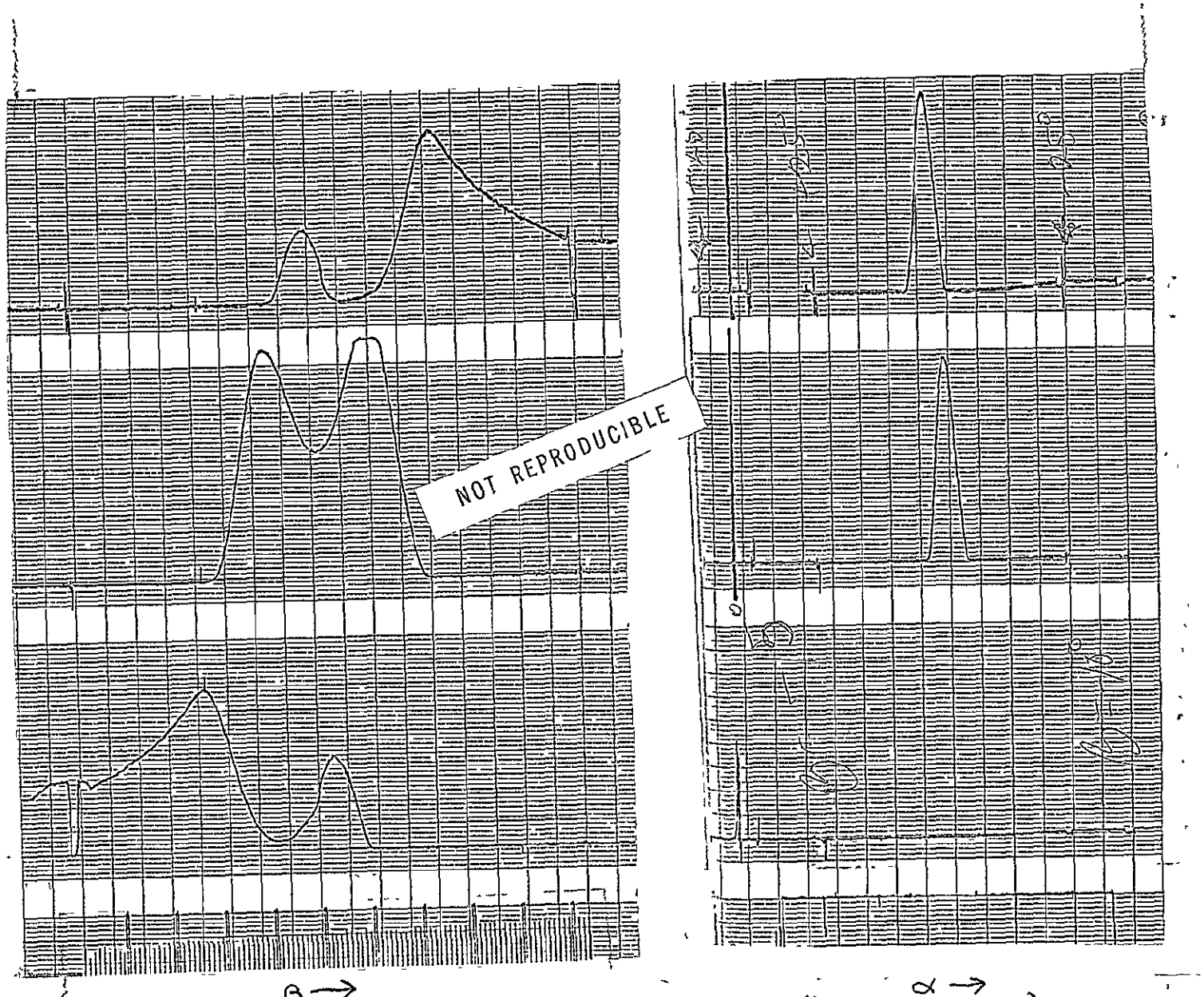


Figure 2. 2
Sample Calibration Curves.

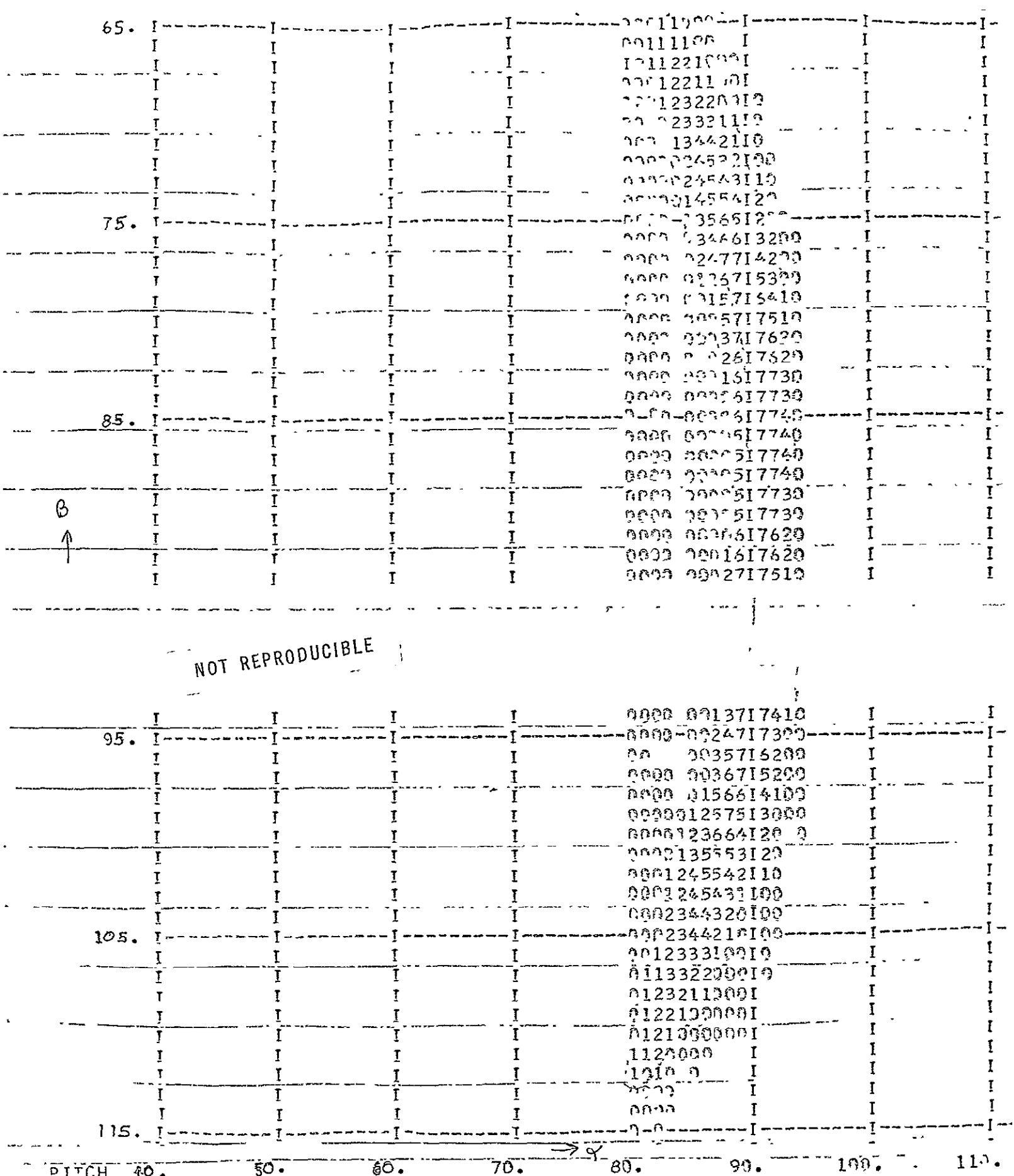


Figure 2.3
Sample Calibration Data Plot

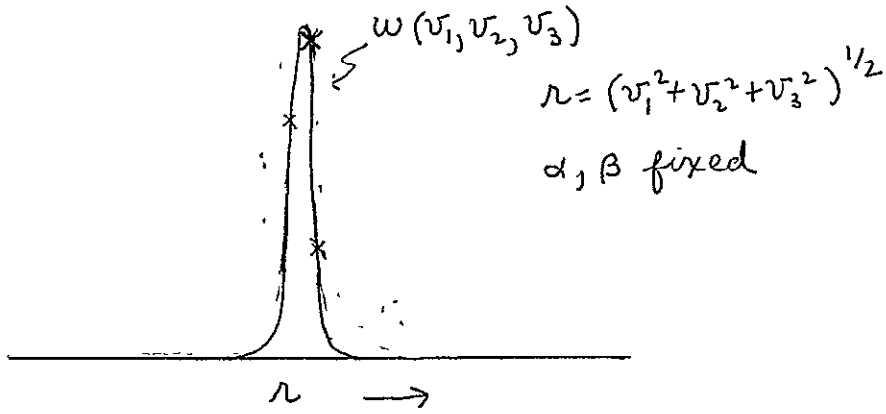


Figure 2.4 Calibration Curve For Increasing $r$, with $\alpha, \beta$ Fixed.

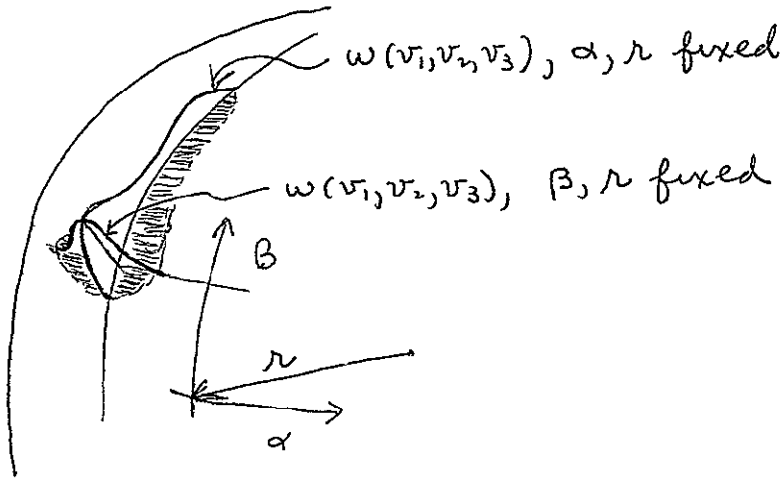


Figure 2.5 Calibration Curves For Fixed $r$.

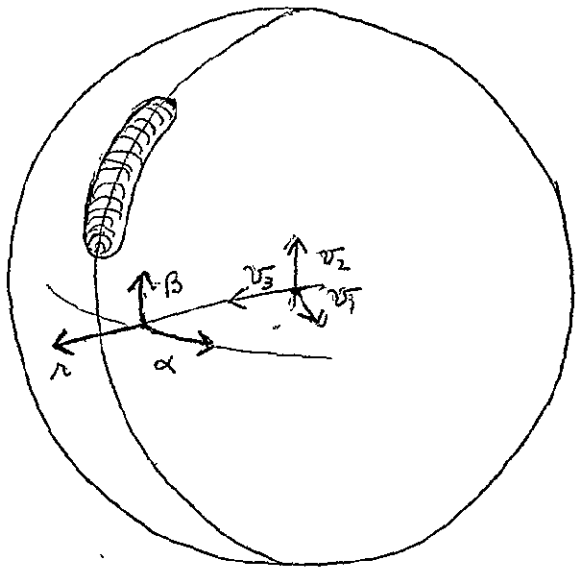


Figure 2-6. Hot Dog Shaped Region $S'$, in Velocity Vector Space For Which $\omega(v_1, v_2, v_3) > 0$

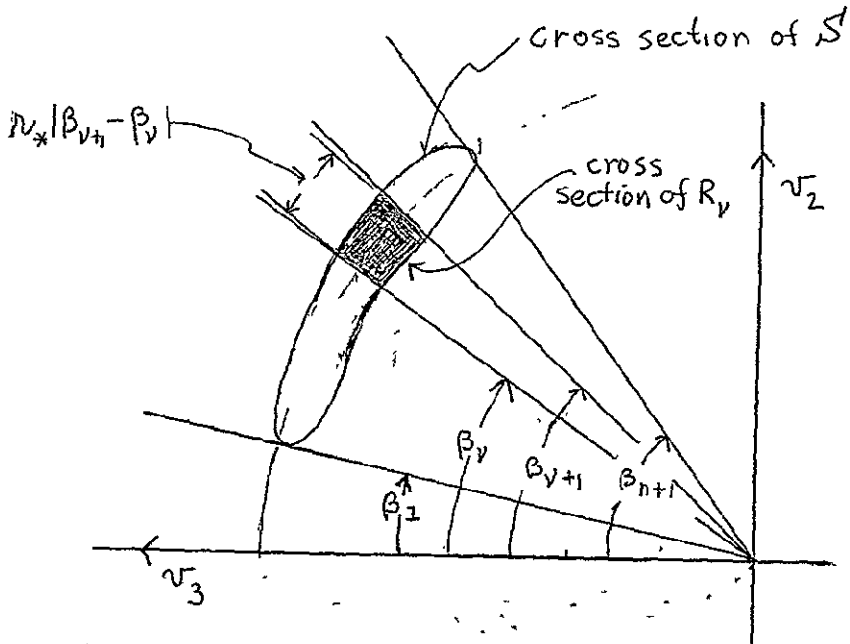


Figure 2.7. Cross Section of $S'$ and $R_\nu$ in Plane of $\alpha = 0$.

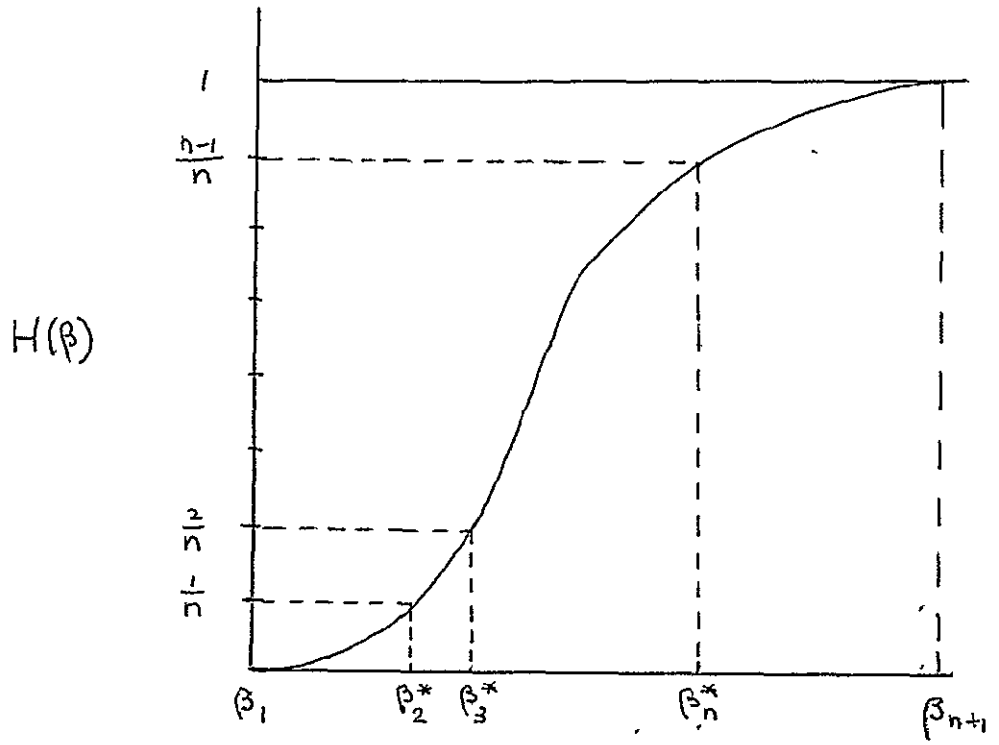


$$H(\beta) = \int_{\beta_1}^{\beta} [h(\beta)]^{1/3} d\beta \Big/ \int_{\beta_1}^{\beta_{n+1}} [h(\beta)]^{1/3} d\beta$$

Figure 28

Graphical Solution of $H(\beta_\nu^*) = \frac{\nu-1}{n}$, $\nu = 2, 3, \ldots, n$

SECTION 3

ESTIMATES OF THE HELIUM FRACTION

## 3.1. Introduction

In this section we briefly present two relatively simple methods for estimating the Helium fraction. The methods are based on the use of the same non-linear least squares parameter estimation program for which the quadrature methods of Section 2 were developed. We only briefly discuss the relative accuracy of these methods as compared to other methods, since it will depend crucially on how well the instrument resolves the proton and $\alpha$-particle distributions. However, a comparative accuracy study should not be hard to perform, given a complete non-linear least squares program with data simulation.

## 3.2. Assumptions and Definitions

The particle velocity vector distribution $f_p(v,\theta_p)$ for protons is assumed to be of the form

$$f_p(v,\theta_p) = \frac{N_p}{(2\pi)^{3/2}} \frac{1}{\prod_{i=1}^{3}\sqrt{\lambda_{ip}}} e^{-\frac{1}{2}(v-\mu_p)\Gamma_p D_{\lambda p}^{-1}\Gamma_p'(v-\mu_p)'} \qquad (3.2.1)$$

where $N_p$ is the proton number density, $\underline{\mu}_p$ is the proton bulk velocity vector, $\Gamma_p$ is an orthogonal matrix and $D_{\lambda p}$ is a diagonal

matrix with diagonal elements $\lambda_{ip}$, $i = 1,2,3$, where

$$\lambda_{ip} = \frac{kT_{ip}}{m_p} \quad , \quad i = 1,2,3 \tag{3.2.2}$$

k is Boltzman's constant, $T_{ip}$ is the proton temperature in the direction determined by the $i^{th}$ column of $\Gamma_p$, and $m_p$ is the proton mass.

If the instrument calibration is performed with a proton beam, then the particle velocity vector distribution of $\alpha$-particles looks to the instrument like $f_\alpha(v,\theta_\alpha)$ given by

$$f_\alpha(v,\theta_\alpha) = \frac{2N_\alpha}{(2\pi)^{3/2}} \frac{1}{\prod_{i=1}^{3} \sqrt{\lambda_{i\alpha}}} e^{-\frac{1}{2}(v-\sqrt{2}\mu_\alpha)\Gamma_\alpha D_{\lambda\alpha}^{-1}\Gamma'(v-\sqrt{2}\mu_\alpha)'} \tag{3.2.3}$$

where $N_\alpha$, $\mu_\alpha$, $\Gamma_\alpha$, $D_{\lambda\alpha}$, $\lambda_{i\alpha}$, $T_{i\alpha}$ and $m_\alpha$ are defined for $\alpha$-particles analogous to the same quantities for protons. Assume now that $\mu_p \overset{\text{def}}{=} \mu_\alpha = \mu$, $\Gamma_p \overset{\text{def}}{=} \Gamma_\alpha = \Gamma$ and $4T_{ip} = T_{i\alpha}$. Then $\lambda_{ip} \overset{\text{def}}{=} \lambda_{i\alpha} = \lambda_i$, since $4m_p = m_\alpha$. Let $g(v,\mu,\Sigma)$ be defined by

$$g(v,\mu,\Sigma) = \frac{1}{(2\pi)^{3/2}|\Sigma|^{1/2}} e^{-(v-\mu)\Sigma^{-1}(v-\mu')} \tag{3.2.4}$$

with $\Sigma = \Gamma D_\lambda \Gamma'$. Then the sum of the two particle velocity vector distributions looks to the instrument like

$$f_p(v,\theta_p)+f_\alpha(v,\theta_\alpha) = N_p\, g(v,\mu,\Sigma)+2N_\alpha\, g(v,\sqrt{2}\mu,\Sigma) \quad . \qquad (3.2.5)$$

Let $w_k(v)$ be the instrument response at the $k^{th}$ combination of collector, energy step and relative instrument position, $k = 1,2,\ldots,n$.[2/] Then the $k^{th}$ data point, or instrument response $I_k$, due to an input (3.2.5) is modeled by

$$I_k = I_k(N_p,N_\alpha,\mu,\Sigma) = N_p \iiint_{-\infty}^{\infty} w_k(v)g(v,\mu,\Sigma)dv + 2N_\alpha \iiint_{-\infty}^{\infty} w_k(v)g(v,\sqrt{2}\mu,\Sigma)dv, \qquad (3.2.6)$$
$$k = 1,2,\ldots,n \quad .$$

3.3. Description of the Method

Let $h_{ki} = h_{ki}(\mu,\Sigma)$, $i = 1,2$, $k = 1,2,\ldots,n$, be defined by

$$h_{k1}(\mu,\Sigma) = \iiint w_k(v)g(v,\mu,\Sigma)dv \qquad (3.3.1)$$
$$h_{k2}(\mu,\Sigma) = 2\iiint w_k(v)g(v,\sqrt{2}\mu,\Sigma)dv \qquad k = 1,2,\ldots,n$$

The system of equations (3.2.6) may be rewritten



[2/] This $n$ is unrelated to $n$ of Section 2, we are running out of symbols.

$$\begin{pmatrix} I_1 \\ I_2 \\ \vdots \\ I_n \end{pmatrix} = \begin{pmatrix} h_{11} & h_{12} \\ h_{21} & h_{22} \\ \vdots & \vdots \\ h_{n1} & h_{n2} \end{pmatrix} \begin{pmatrix} N_p \\ N_\alpha \end{pmatrix} = N \begin{pmatrix} h_{11} & h_{12} \\ h_{21} & h_{22} \\ \vdots & \vdots \\ h_{n1} & h_{n2} \end{pmatrix} \begin{pmatrix} (1-\delta) \\ \delta \end{pmatrix} \qquad (3.3.2)$$

where $N = N_p+N_\alpha$ , and $\delta = N_\alpha(N_p+N_\alpha)$ .

3.3.1. Equations for Method 1

Let $H = H(\mu,\Sigma)$ be the $n \times 2$ matrix with $ki^{th}$ entry $h_{ki}$. If $\mu,\Sigma$ are assumed, and the data $I_1,\ldots,I_n$ are given, then, using (3.3.2), the least squares estimates $\hat{N}_p$ and $\hat{N}_\alpha$ for $N_p$ and $N_\alpha$ are given by

$$\begin{pmatrix} \hat{N}_p \\ \hat{N}_\alpha \end{pmatrix} = (H'H)^{-1}H' \begin{pmatrix} I_1 \\ \vdots \\ I_n \end{pmatrix} , \quad H = H(\mu,\Sigma) \quad . \qquad (3.3.3)$$

The Helium fraction $\delta$ is estimated by $\hat{N}_\alpha/(\hat{N}_p+\hat{N}_\alpha)$.

3.3.2. Equation for Method 2

If $N$, $\mu,\Sigma$ and $I_1,\ldots,I_n$ are given, the least squares estimate $\hat{\delta}$ for $\delta$ is, from (3.3.2)

$$\hat{\delta} = \frac{1}{\sum_{i=1}^{n}(h_{i2}-h_{i1})^2} \frac{1}{N} \sum_{i=1}^{n}(I_i-h_{i1})(h_{i2}-h_{i1}) \quad . \qquad (3.3.4)$$

3.3.3. The Procedures

Procedure for Method 1: Obtain starting values for $\mu$ and $\Sigma$ by the use of the non-linear least squares program with $N_\alpha$ assumed 0. [Delete all obvious 100% $\alpha$-particle data from the data set.] Using these $\mu$ and $\Sigma$, determine $\hat{N}_p$ and $\hat{N}_\alpha$ via (3.3.3). Introduce the model

$$f_p(v,\theta_p)+f_\alpha(v,\theta_\alpha) = \hat{N}_p g(v,\mu,\Sigma) + \hat{N}_\alpha \cdot 2g(v,\sqrt{2}\mu,\Sigma) \qquad (3.3.5)$$

into the non-linear least squares program with $\hat{N}_p$ and $\hat{N}_\alpha$ fixed, and $\mu$, $\Sigma$ as parameters to be fitted. Using the updated estimates of $\mu$ and $\Sigma$, obtain new $\hat{N}_p$ and $\hat{N}_\alpha$ from (3.3.3).

Procedure for Method 2: Obtain starting guesses for $N$, $\mu$, and $\Sigma$ as in Method 1. (Starting guess for $N$ = starting guess for $N_p$). Using these values for $N$, $\mu$ and $\Sigma$ estimate $\delta$ by the use of (3.3.4). Iterate, if necessary by replacing $\hat{N}_p$ and $\hat{N}_\alpha$ by $N(1-\hat{\delta})$ and $N\hat{\delta}$ in (3.2.5) with $N$ a free parameter and $\hat{\delta}$ fixed.

## 3.4. Conclusion

Either method is simple, assuming the existence of auxiliary programs which must be developed in any case. The general model (3.2.5) with all parameters to be determined may also, of course, be used in the non-linear least squares program. In the case where the two distributions are poorly resolved by the instrument, then there is some reason to believe that either of the above methods, particularly Method 2 if $\delta$ is small, would tend to be more stable than fitting the full general model simultaneously.

For the case of the two distributions resolved to the extent that two distinct peaks are identifiable, these methods should be compared with methods based on the relative peak heights, etc. For the case of the distributions completely resolved, $N_\alpha$ may be estimated in a least squares sense by $\hat{N}_\alpha$ given by

$$\hat{N}_\alpha = \frac{\sum_k I_k h_{k2}}{\sum_k h_{k2}^2} \tag{3.4.1}$$

where the summation is taken only over $k$ for which $I_k$ contains no contribution from protons, and $\mu$ and $\Sigma$ are determined independently from the proton data.

SECTION 4

# LINEAR ESTIMATES OF PLASMA PARAMETERS

## 4.1. Introduction

Linear estimates of the plasma parameters (for data from protons only) can be made, because the parameters are simple functions of the moments, which can be viewed as linear functionals. The linear estimates can be expected not to be as accurate as the non-linear estimates when the Maxwellian distribution holds, since the latter uses a known functional form for the particle velocity vector distribution. However, the linear estimates will be cheap to compute, since the coefficients can be calculated ahead of time. Also the linear estimates of the moments are reasonable estimates of the moments irrespective of the true nature of the particle velocity vector distribution. Their accuracy (not counting the errors induced by poor calibration data) may be examined ahead of time by simulation.

Let $f(v,\theta)dv$ be the particle velocity vector distribution, where $\theta$ stands for the parameter set $\theta = \{N, \mu, \Sigma\}$, as defined in previous sections and $v = (v_1, v_2, v_3)$. (We are assuming data from protons only).

If

$$f(v,\theta) = \frac{N}{(2\pi)^{3/2}\,|\Sigma|}\, e^{-\frac{1}{2}(v-\mu)\Sigma^{-1}(v-\mu)'} \qquad (4.1.1)$$

then

$$N = \iiint f(v,\theta)dv \quad = \text{number density}$$

$$\mu_i = \frac{1}{N}\iiint v_i f(v,\theta)dv \ , \ i = 1,2,3 = \text{coordinates of bulk velocity vector (4.1.2)}$$

$$\sigma_{ij} = \frac{1}{N}\iiint v_i v_j f(v,\theta)dv - \mu_i\mu_j \quad = \text{entries of the pressure tensor, } \Sigma = \{\sigma_{ij}\} .$$

As before, let $w_k(v)$, $k = 1,2,\ldots,n$, be the current at the output of the target at the $k^{th}$ observation step due to a cold proton beam of unit number density and velocity vector $v$. The observed data points $I_k$, $k = 1,2,\ldots,n$, (that is, current at the output of the target) are given by

$$I_k = \iiint w_k(v) f_\theta(v)dv \quad , k = 1,2,\ldots,n. \tag{4.1.3}$$

It will be convenient to use the inner produce notation $(f,g)$,

$$(f,g) = \iiint f(v)g(v)dv \ . \tag{4.1.4}$$

Let

$$\begin{aligned} g_o(v) &= 1 \\ g_i(v) &= v_i \quad , i = 1,2,3 \\ g_{ij}(v) &= v_i v_j \quad , i,j = 1,2,3 \ . \end{aligned} \tag{4.1.5}$$

Then, writing $f_\theta$ for the function of $v$ defined by $f(v,\theta)$.

$$\begin{aligned} N &= (g_0, f_\theta) \\ N\mu_i &= (g_i, f_\theta) \quad i = 1,2,3 \\ N(\sigma_{ij}+\mu_i\mu_j) &= (g_{ij}, f_\theta) \quad . \end{aligned} \tag{4.1.6}$$

We will find linear least squares estimates of the 10 quantities

$$N;\ N\mu_i,\ i = 1,2,3\ ;\ N(\sigma_{ij}+\mu_i\mu_j),\ i \le j = 1,2,3.$$

Estimates of the parameters $N$, $\mu_i$ and $\sigma_{ij}$ can then be computed from these quantities.

## 4.2. The Method in One Dimension

To help in understanding the method as well as its pitfalls, we describe it in some detail for functions defined on the (one-dimensional) real line, as opposed to 3-dimensional velocity vector space.

In one dimension we wish to estimate

$$\begin{aligned} N &= \int \tilde{g}_0(v) f(v,\theta)dv \qquad \tilde{g}_0(v) \equiv 1 \\ \mu N &= \int \tilde{g}_1(v) f(v,\theta)dv \qquad \tilde{g}_1(v) = v \\ N(\sigma^2+\mu^2) &= \int \tilde{g}_2(v) f(v,\theta)dv \qquad \tilde{g}_2(v) = v^2 \ . \end{aligned} \tag{4.2.1}$$

See Figure 4.1. In order to carry out the method we must have a finite region of integration outside of which $f(v,\theta)$ is known to be always negligible. Call this region R. We will let

$$(f,g) = \int_R f(v)g(v)dv \quad . \tag{4.2.2}$$

Let $\mathcal{H}_n$ be the (assumed n-dimensional) linear space of all finite linear combinations of the functions $\{w_k(v)\}_{k=1}^{n}$. Let us comceptually approximate $\tilde{g}_i(v)$ by an element $\hat{\tilde{g}}_i(v)$ in the space $\mathcal{H}_n$, (i = 0,1,2).

$$\hat{\tilde{g}}_i(v) = \sum_{k=1}^{n} c_{ik}w_k(v) \tag{4.2.3}$$

where the $\{c_{ik}\}$ are to be found. Choose the $\{c_{ik}\}$ to minimize

$$\|\tilde{g}_i(v) - \hat{\tilde{g}}_i(v)\|^2 = \int_R \left(\tilde{g}_i(v) - \sum_{k=1}^{n} c_{ik}w_k(v)\right)^2 dv \tag{4.2.4}$$

$$= \int_R \tilde{g}_i(v) - 2\sum_{k=1}^{n} c_{ik}a_{ik} + \sum\sum_{k\ell} c_{ik}c_{i\ell}b_{k\ell}$$

where

$$a_{ik} = \int_R \tilde{g}_i(v)w_k(v)dv \qquad i = 0,1,2$$
$$b_{k\ell} = \int_R w_k(v)w_\ell(v)dv \quad . \tag{4.2.5}$$

The coefficients $(c_{i1},c_{i2},\ldots,c_{in})$ which minimize (4.2.4) are easily shown to be given by

$$(c_{i1},c_{i2},\ldots,c_{in}) = (a_{i1},a_{i2},\ldots,a_{in})B^{-1} \qquad (4.2.6)$$

where $B$ is the $n \times n$ symmetric matrix with $k\ell^{th}$ entry $b_{k\ell}$. $B$ will be diagonal if the instrument "windows" do not overlap (in velocity vector space). Note that $\hat{g}_i(v)$ will approximate $\tilde{g}_i(v)$ very nicely in the region of interest if the $\{w_k(v)\}$ are as in Figure 4.1 but not so well if they are as in Figure 4.2. See Figures 4.3 and 4.4.

Once the coefficients $(c_{i1},c_{i2},\ldots,c_{in})$, $i = 0,1,2$, are chosen, we approximate the desired moment

$$\int_R \tilde{g}_i(v)f(v,\theta)dv \qquad (4.2.7)$$

by

$$\int_R \hat{g}_i(v)f(v,\theta)dv = \sum_{k=1}^{n} c_{ik}\int w_k(v)f(v,\theta)dv = \sum_{k=1}^{n} c_{ik}I_k \quad , \qquad (4.2.8)$$

$$i = 0,1,2 \ .$$

An error bound is given by the formula

$$\left|\int_R \tilde{g}_i(v)f(v,\theta)dv - \sum_{k=1}^{n} c_{ik}I_k\right| = \left|\int_R (\tilde{g}_i(v)-\hat{g}_i(v))f(v,\theta)dv\right|$$

(Cauchy-Schwartz Inequality)

$$\leq \left[\int_R (\tilde{g}_i(v)-\hat{\tilde{g}}_i(v))^2 dv \cdot \int_R f^2(v,\theta)dv\right]^{1/2} = \|\tilde{g}_i(v)-\hat{\tilde{g}}_i(v)\|^{1/2} \|f(v,\theta)\|^{1/2} \tag{4.2.9}$$

Note that the function

$$\hat{f}(v,\theta) = \sum_{k=1}^{n} f_k w_k(x) \tag{4.2.10}$$

where

$$(f_1,f_2,\ldots,f_n) = (I_1(\theta),\ldots,I_n(\theta))B^{-1} \tag{4.2.11}$$

is an approximation to $f(v,\theta)$ in $\mathcal{H}_n$ and satisfies

$$(\tilde{g}_i(v)-\hat{\tilde{g}}_i(v),\ \hat{f}(v,\theta)) = 0 \quad . \tag{4.2.12}$$

Hence we may replace the right hand side of (4.2.9) by

$$\int_R (\tilde{g}_i(v)-\hat{\tilde{g}}_i(v))(f(v,\theta)-\hat{f}(v,\theta))dv$$

$$\leq \|\tilde{g}_i(v)-\hat{\tilde{g}}_i(v)\|^{1/2} \|f(v,\theta)-\hat{f}(v,\theta)\|^{1/2} \quad .$$

Of course $\|f(v,\theta)-\hat{f}(v,\theta)\|^{1/2}$ is not generally known in advance. Thus the error bound for the moment estimates depend on how well $\tilde{g}_i(v)$ and $f(v,\theta)$ may be approximated by linear combinations of the window functions $\{w_k(v)\}_{k=1}^{n}$ .

## 4.3. The Estimates in Velocity Vector Space

The formulas are unchanged for three dimensional space. It is necessary to establish numerically from the calibration data the quantities

$$a_{ok} = \iiint_R w_k(v)dv \qquad k = 1,2,\ldots,n$$

$$a_{1k}^{(j)} = \iiint_R v_j w_k(v)dv \qquad j = 1,2,3, \quad k = 1,2,\ldots,n \tag{4.3.1}$$

$$a_{2k}^{(i,j)} = \iiint_R v_i v_j w_k(v)dv \quad , \; i,j = 1,2,3, \quad k = 1,2,\ldots,n$$

which play the role of $a_{ok}$, $a_{1k}$ and $a_{2k}$ in (4.2.5), and

$$b_{k\ell} = \iiint_R w_k(v) w_\ell(v)dv \qquad . \tag{4.3.2}$$

These are independent of observed data, of course, and are only calculated once. The coefficients $(c_{o1},c_{02},\ldots,c_{on}),\ldots$ $(c_{21}^{(i,j)},c_{22}^{(i,j)},\ldots,c_{2n}^{(i,j)})$ used in estimating the moments, analogous to (4.2.7) and (4.2.8) are given by (4.2.6).

## 4.4. Conclusions

Clearly the accuracy of the method depends on the particular instrument design as well as the unknown particle velocity vector distribution. Errors in the calibration data and in the quantities

(4.3.1) and (4.3.2) will also affect the results.

It is recommended that a pilot check of the accuracy of the method be made as follows. A set of test cases $f(v,\theta)$ are chosen, (most reasonably Maxwellian). To study errors due to the method (as opposed to errors due to faulty calibration data, the $w_k(v)$ may be defined by smoothed calibration data. Using an accurate quadrature procedure, the quantities in (4.3.1) and (4.3.2) are calculated. The "data" $I_k$ should be simulated via the same calibration data and quadrature procedure

$$I_k = \iiint w_k(v) f(v,\theta) dv \quad . \tag{4.4.1}$$

The moments and parameters are then estimated via (4.1.5), (4.1.6) and the appropriate 3 dimensional analogue of (4.2.7) and (4.2.8) obtained by erasing the "~" in $\tilde{g}_i$ and $\hat{\tilde{g}}_i$.

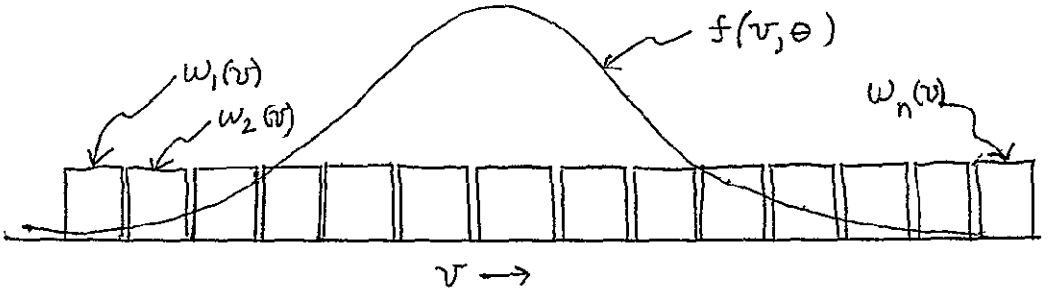


Figure 4-1 Idealized Set of Windows $\{w_R(v)\}$

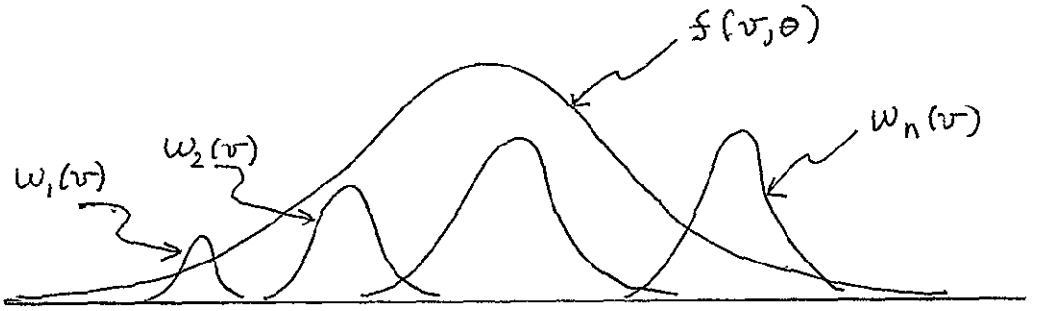


Figure 4-2 Actual Set of Windows, With Gaps, Overlaps, and Varying Sizes

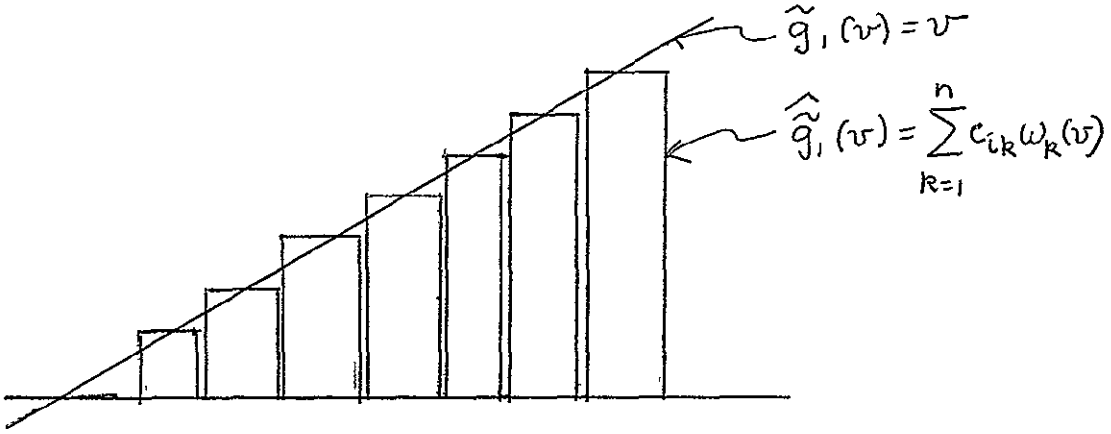


Figure 4-3. Approximation of $\tilde{g}_1(v)$ By Linear Combinations of Idealized Windows

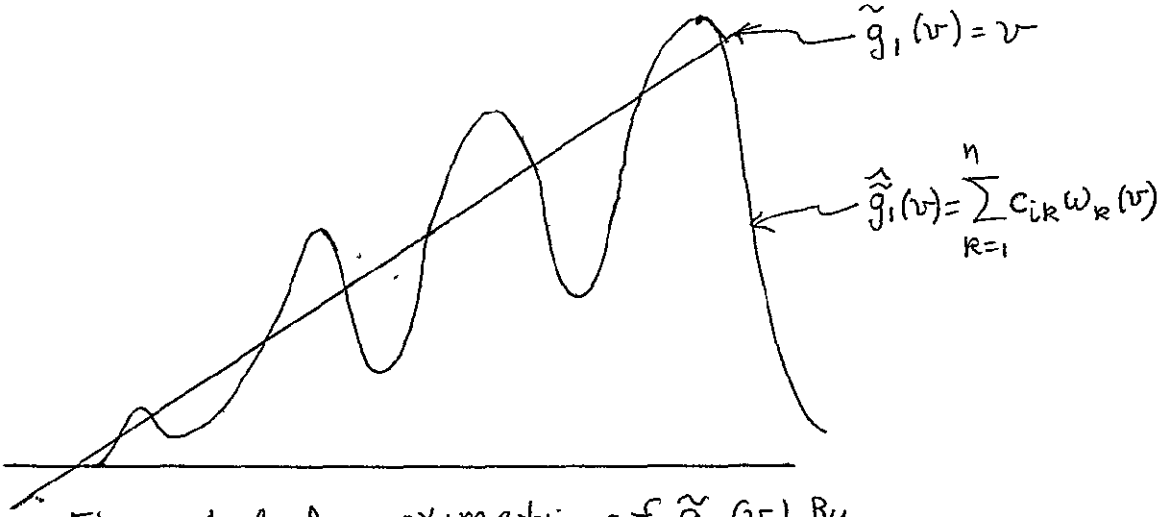


Figure 4-4. Approximation of $\tilde{g}_1(v)$ By Linear Combinations of Actual Windows

# SECTION 5

# CONCLUSIONS

1. Optimization of Numerical Quadrature. Probably the most difficult and time consuming part of the development of any accurate quadrature procedure using a minimal number of quadrature points is the determination of the volumes $\iiint_{R_v} w(v)dv$ or $\iiint_{S} w(v)dv$, of the calibration curves. Once this work is organized on the computer then the development of optimal quadrature formulae as described in Section 2 is not much more if any additional effort. If a quadrature routine is to be used for standard production work over a long period of time, it is probably worth the investment to optimize this routine.

The discussion of this section has illustrated an appropriate and relatively simple way to use the calibration data in the quadrature routine.

2. An Alternative Procedure is described for estimating the Helium fraction. It will require some simulation to compare this procedure against other candidates. It is probably more stable than estimating the Helium fraction simultaneously with the other parameters in the non-linear least squares program.

3. A method for obtaining estimates of the plasma parameters without iteration has been given. While this method is no doubt cheaper than iterative non-linear least squares methods, its accuracy has not been established here. It may be used, however, to provide starting guesses for an iterative method. Furthermore, it provides reasonable estimates of the moments of the distribution irrespective of its functional form, and thus may provide some descriptive numbers when the distribution is not Maxwellian.

SECTION 6

APPENDICES

APPENDIX A

Upper Bounds on the Mixed Partial Derivatives
of The Maxwellian Density

Let

$$f(v,\theta) = \frac{N}{(2\pi)^{3/2}|\Sigma|^{1/2}} e^{-\frac{1}{2}(v-\mu)^{-1}(v-\mu)'} \qquad A.1$$

where $\theta = (N,\mu,\Sigma)$, $v = (v_1,v_2,v_3)$, a velocity vector. We show that

$$\max_{v_1,v_2,v_3,\theta,i,j} \left|\frac{\partial^2 f}{\partial v_i \partial v_j}\right| \leq M \qquad A.2$$

where

$$M = \frac{N}{(2\pi)^{3/2} \prod_{i=1}^{3} \sqrt{\lambda_i}} \frac{1}{\lambda_{min}} \qquad A.3$$

where $\lambda_{min}$ is the smallest among $(\lambda_1,\lambda_2,\lambda_3)$, the eigenvalues of the pressure tensor $\Sigma$.

Represent $\Sigma$ as $\Gamma D_\lambda \Gamma'$ where $\Gamma$ is orthogonal and $D_\lambda$ is diagonal with $ii^{th}$ entry $\lambda_i = \frac{kT_i}{m}$. Let

$$g(x) = e^{-\frac{1}{2}\sum_{i=1}^{3}\frac{x_i^2}{\lambda_i}}, \quad x = (x_1,x_2,x_3) . \qquad A.4$$



6

Then

$$f(v,\theta) = \frac{N}{(2\pi)^{3/2} \prod_{i=1}^{3} \sqrt{\lambda_i}} \; g(x) \qquad \text{A.5}$$

with

$$x = (v-\mu)\Gamma \qquad \text{A.6}$$

$(\prod_{i=1}^{3} \sqrt{\lambda_i} = |\Sigma|^{1/2})$.

Since the Jacobian of the above transformation from $v$ to $x$ is 1 then

$$\max \left| \frac{\partial^2 f}{\partial v_i \partial v_j} \right| = \max \left| \frac{\partial^2 g}{\partial x_i \partial x_j} \right| \times \frac{N}{(2\pi)^{3/2} \prod_{i=1}^{3} \sqrt{\lambda_i}} \; . \qquad \text{A.7}$$

The maximum curvature of $g$ occurs at $x_1 = x_2 = x_3$, in the direction of the $x_k$ axis where $\lambda_k$ is the smallest among $\lambda_1, \lambda_2, \lambda_2$ , and so

$$\max_{i,j,x_i,x_j} \left| \frac{\partial^2 g}{\partial x_i \partial x_j} \right| = \left. \frac{\partial^2 g}{\partial x_k^2} \right|_{x_1=x_2=x_3=0} = \frac{1}{\lambda_k} \qquad \text{A.8}$$

since

$$\left. \frac{\partial^2}{\partial x_k^2} \; e^{-\frac{x_k^2}{2\lambda_k}} \right|_{x_k=0} = \frac{1}{\lambda_k} \; . \qquad \text{A.9}$$

It is obvious that if $f(v,\theta)$ is the sum of 2 Maxwellian distributions, as in (3.2.5), then A.3 holds with N replaced by $N_p+2N_\alpha$.

## APPENDIX B

### Jensen's Inequality

Let $g(x)$ be any strictly convex function of the real variable $x$, and let $x_1, x_2, \ldots, x_n$ be any given $n$ real numbers in the domain of $g$, with

$$\bar{x} = \frac{1}{n} \sum_{\nu=1}^{n} x_\nu \quad . \tag{B.1}$$

Then,

$$\sum_{\nu=1}^{n} g(x_\nu) \geq n g(\bar{x}) \tag{B.2}$$

with equality holding if and only if $x_\nu = \bar{x}$, $\nu = 1,2,\ldots,n$ .

Proof:

The straight line $y(x)$ given by

$$y(x) = g'(\bar{x})(x-\bar{x})+g(\bar{x}) \tag{B.3}$$

is tangent to the strictly convex function $g(x)$ at the point $x = \bar{x}$ and is below $g(x)$ otherwise. Thus

$$\sum_{\nu=1}^{n} g(x_\nu) \geq g'(\bar{x}) \sum_{\nu=1}^{n} (x_\nu-\bar{x}) + n g(\bar{x}) = n g(\bar{x})$$

with equality holding if and only if $x_\nu = \bar{x}$, $\nu = 1,2,\ldots,n$.

To apply Jensen's inequality to (2.2.8), set $g(x) = x^{5/3}$,

$$x_\nu = \iiint_{R_\nu} w^{3/5}(v)dv, \quad \text{and to apply to (2.4.4) set } g(x) = x^3 ,$$

$$\bar{x}_\nu = \int_{\beta_\nu}^{\beta_{\nu+1}} [h(\beta)]^{1/3} d\beta .$$

## APPENDIX C

### Proof of the Inequality in (2.4.8)

We show that

$$\sum_{\nu=1}^{n} (\beta^*_{\nu+1}-\beta^*_{\nu})^2 \int_{\beta^*_{\nu}}^{\beta^*_{\nu+1}} h(\beta)d\beta - \frac{1}{n^2}\left[\int_{\beta_1}^{\infty_{n+1}} [h(\beta)]^{1/3}d\beta\right]^3$$

$$\leq \sum_{\nu=1}^{n} |\beta^*_{\nu+1}-\beta^*_{\nu}|^4 \max_{\theta\epsilon(\beta^*_{\nu},\beta^*_{\nu+1})} |h'(\theta)| \qquad \text{C.1}$$

where the $\beta^*_{\nu}$ satisfy

$$\int_{\beta^*_{\nu}}^{\beta^*_{\nu+1}} [h(\beta)]^{1/3}d\beta = \frac{1}{n}\int_{\beta_1}^{\beta_{n+1}} [h(\beta)]^{1/3}d\beta \quad . \qquad \text{C.2}$$

Proof:

If the $\{\beta^*_{\nu}\}$ satisfy the above condition, then, according to Jensen's Inequality

$$\frac{1}{n^2}\left[\int_{\beta_1}^{\beta_{n+1}} [h(\beta)]^{1/3}d\beta\right]^3 = \sum_{\nu=1}^{n}\left[\int_{\beta_{\nu}}^{\beta^*_{\nu+1}} [h(\beta)]^{1/3}d\beta\right]^3 \qquad \text{C.3}$$

where we are writing $\beta^*_1 = \beta_1$, $\beta^*_{n+1} = \beta_{n+1}$.

Thus, it is only necessary to show that

$$(\beta^*_{\nu+1}-\beta^*_\nu)^2 \int_{\beta^*_\nu}^{\beta^*_{\nu+1}} h(\beta)d\beta \; - \left[\int_{\beta^*_\nu}^{\beta^*_{\nu+1}} [h(\beta)]^{1/3}d\beta\right]^3 \qquad \text{C.4}$$

$$\leq \max_{\theta\epsilon(\beta_\nu,\beta_{\nu+1})} |h'(\beta)| \; (\beta^*_{\nu+1}-\beta^*_\nu)^4.$$

By the mean value theorem, there exists a $\bar{\beta}_\nu$ between $\beta^*_\nu$ and $\beta^*_{\nu+1}$ such that

$$(\beta^*_{\nu+1}-\beta^*_\nu)\; h^{1/3}(\bar{\beta}_\nu) \;=\; \int_{\beta^*_\nu}^{\beta^*_{\nu+1}} [h(\beta)]^{1/3}\, d\beta \qquad \text{C.5}$$

and so

$$(\beta^*_{\nu+1}-\beta^*_\nu)^3 h(\bar{\beta}_\nu) \;=\; \left[\int_{\beta^*_\nu}^{\beta^*_{\nu+1}} [h(\beta)]^{1/3}\, d\beta\right]^3 . \qquad \text{C.6}$$

Now

$$h(\beta) \;=\; h(\bar{\beta}_\nu) + (\beta-\bar{\beta}_\nu)\; h'(\xi) \qquad \text{C.7}$$

where $\xi\;\epsilon(\beta_\nu,\beta_{\nu+1})$, and so

$$|h(\beta) - h(\bar{\beta}_\nu)| \;\leq |\beta^*_{\nu+1} - {}^*\beta_\nu| \max_{\theta\epsilon(\beta^*_\nu,\beta_{\nu+1})} h'(\theta) . \qquad \text{C.8}$$

Substituting (C.6), (C.7) and (C.8) into (C.4) gives the result.